saturase), DNA ligase III, and Rad (Ras-related associated with diabetes). There were also down-regulation in 18s and 28s rRNA levels. .

We used real-time PCR analysis to confirm the changes in gene expression observed using the microarray assay. We found that real-time PCR analysis showed alterations in expression similar to those observed in the microarray assay for a number of genes (Fig. 3), yet the increase in change in expression levels was not exactly the same between the 2 assays.

DISCUSSION

The present study is, to our knowledge, the first to examine the effect of a physiologically relevant concentration of genistein on gene expression using microarray analysis. Many
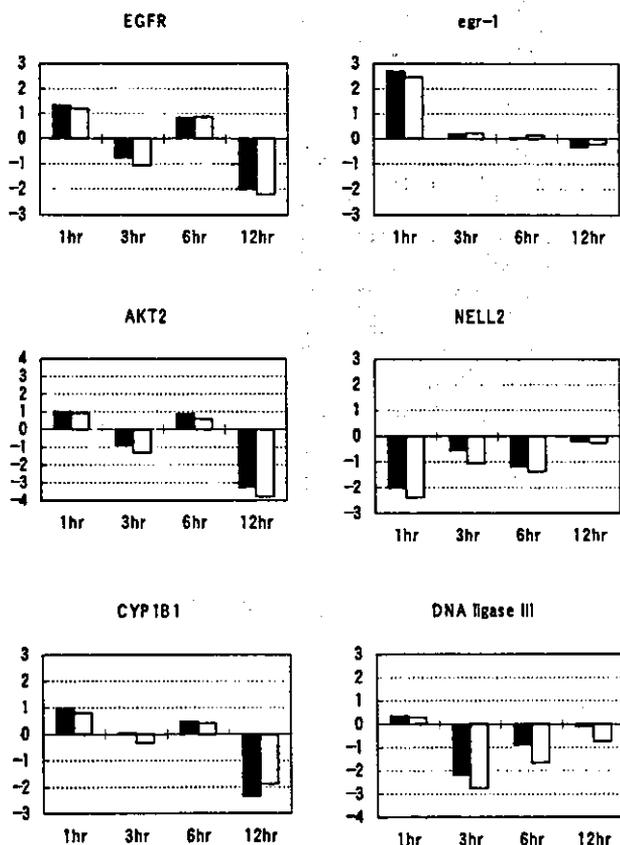

FIGURE 3. The real-time PCR analyses (▨) for the checked 6 genes were in agreement with the microarray data (■). The same RNA used in microarray is used in the real-time PCR. The y-axis indicates the log 2 transformed ratio of mRNA expression, which was compared with the vehicle-treated control group. The fluctuations of mRNA expression in Panc 1 cells treated with 10 μmol/L genistein for 1, 3, 6, and 12 hours are in these 2 different analytic methods, although the increase in change in expression levels is not exactly the same.

researchers choose 50 μmol/L because lower doses of genistein did not cause observable changes in cell proliferation. However, 10 μmol/L is the high end of physiologically achievable genistein, so we chose to carry out a microarray analysis of cells exposed to this level.

In tissue culture experiments, the condition of cells is critical since subtle growth differences can greatly influence gene expression profiles. Hughes et al[12] identified a number of transcripts that exhibited inherent fluctuation in isogenic untreated yeast cultures that appeared to have no phenotypic differences. Taking this into account, only genes that showed more than a fourfold change in expression by genistein were chosen for further analysis in the present study.

We found that genistein altered the expression of a number of genes known to be involved in the epidermal growth factor pathway, namely EGF-R, egr-1, AKT2, CYP1B1, and NELL2.

Genistein is a protein tyrosine kinase inhibitor. Tyrosine kinase activity of EGF-R is directly responsible for most cellular events mediated by EGF.[13] EGF-R is overexpressed in many malignancies, including pancreatic cancer, from which Panc 1 cells are derived. In breast cancer, intrinsic or acquired resistance to antiestrogens is often associated with elevated expression of EGF-R.[14] Dalu et al[15] found that genistein inhibited EGF-R expression in the rat dorsolateral prostate.

AKT2 can be activated by EGF, and overexpression of AKT2 contributes to the malignant phenotype in a subset of human ductal pancreatic cancers.[16] AKT2 up-regulation can be considered a self-protective mechanism after exposure to stress stimuli.[17] Our observed lowering of AKT2 expression by genistein suggests that it disables protective mechanisms in cancer cells.

egr-1 is also an important member of the EGF signaling cascade.[18] egr-1 gene expression has been monitored in many cell types in response to mitogens[19] and has also been connected with development of human cancers. Overexpression of egr-1 has been observed in the majority of human prostate cancer.[20] In our study, the expression profile of egr-1 matched the reported immediate early transcription of egr-1,[21] indicating that the microarray chip hybridization data concur with data generated using other methods. This conclusion is also supported by the expression profiles of FOS and FOSB in the current study, which match previous reports showing they are usually induced within 15 minutes and became undetectable after 1 hour.[22]

NELL2 contains EGF-like repeats and is a member of the epidermal growth factor gene family.[23] Others have shown NELL2 mRNA is abundantly expressed in Burkitt lymphoma, Raji cells, and colorectal adenocarcinoma SW480 cells.[24] Our observation that genistein inhibited NELL2 expression would likely result in decreased EGF signaling.

A role for cytochrome P-450 has been identified in the EGF-R signaling pathway.[25] Cells with active P-450 demon-

strated marked increases in both the extent and sensitivity of DNA synthesis in response to EGF. CYP1B1 belongs to the multigene family cytochrome P-450, which can influence the response of established tumors to anticancer drugs by metabolizing those drugs.[26] CYP1B1 shows increased expression in a wide range of human tumors, including breast and colon cancers and is specifically located in tumor cells.[27] Cytochrome P-450 can deactivate a wide variety of environmental chemicals and can thus can be considered as a self-protecting mechanism. Inhibition of CYP1B1 expression further suggests genistein can disable cancer cell protective mechanisms.

In addition to repression of a number of genes related to EGF signaling, we also observed that genistein inhibited expression of DNA ligase III, which plays an important role in DNA replication, recombination, and repair. After exposure to DNA-damaging agents, such as topoisomerase inhibitor, cell death signals are initiated. Genistein has been reported to inhibit topoisomerase II activity both in vitro and in vivo.[28,29] In addition to its structural role in restoring the integrity of the nuclear genome, DNA ligase III also plays an important role in fine-tuning the trigger point of the cell death cascade.[30] Our observation that genistein inhibited DNA ligase III gene expression suggests that genistein may block DNA replication, recombination, and repair in cancer cells.

In human breast cancer and melanoma cells, Rad acts to increase serum-stimulated DNA synthesis.[31] Although a decrease in Rad expression may decrease DNA synthesis, it increases the ability of cells to recruit glucose, which facilitates cancer growth.[32] However, Boros et al[33] reported that genistein could shift glucose carbons from cell proliferation–related structural and functional macromolecules (eg, RNA, DNA), which are synthesized through nonoxidative pathways, to direct oxidative degradation of glucose and thus diminished proliferation and survival of pancreatic adenocarcinoma cells in culture. Inhibiting the formation of ribose from glucose blocks ribosome formation and is one of the important underlying mechanisms by which genistein regulates tumor cell growth.[34] Consistent with those findings, the present study showed that genistein lowered levels of 18s and 28s rRNA after 12 hours. Lower 18s and 28s rRNA levels would not only reduce protein synthesis in general but also enhance the effect of genistein-lowering levels of specific mRNA species.

SCD overexpression is associated with genetic predisposition to hepatocarcinogenesis in mice and rats.[35] Overexpression of SCD has also been reported in rat mammary carcinomas, and sterculic acid, an SCD activity inhibitor, inhibits rat mammary carcinogenesis.[36] The possibility of SCD involvement in mammary carcinogenesis is strengthened by a case-control study suggesting a decreased risk of breast cancer in women with low SCD enzyme activity.[37] High SCD activity has been implicated in a wide range of disorders including diabetes, atherosclerosis, obesity, and viral infection. Our observation that genistein lowered SCD expression might explain

the difference in the incidence of these diseases between Asian and Western populations.[38,39]

IL-8 has recently been shown not only to be overexpressed in various human cancers and cancer cell lines but also to contribute to human cancer progression.[40] Elevated IL-8 secretion may not only directly stimulate tumor cell proliferation but may also support tumor mass expansion via direct or indirect induction of tumor vessel formation.[41] Although IL-8 is associated with cancer progression, here we found that IL-8 gene expression was up-regulated about fivefold after 3 hours genistein treatment. This may explain why physiological levels of genistein can stimulate growth of solid tumors.[42] Thus, it appears genistein may be useful in preventing carcinogenesis but not useful as a chemotherapeutic agent for solid tumors.

In conclusion, the current data suggest genistein may inhibit carcinogenesis in several ways. The most obvious way is by interfering with the EGF-R signaling pathway. In addition, genistein appears capable of disabling cancer cell self-protective mechanisms. Furthermore, genistein may inhibit carcinogenesis by inhibiting DNA repair mechanisms. Finally, our data support findings indicating that genistein inhibits rRNA formation, which is an important mechanism by which genistein regulates tumor cell growth.

However, this work only addressed to cancer cells in vitro. Any attempt to apply this conclusion to normal cells or in vivo should be made with caution. Further experiments focusing on those aspects are needed.

REFERENCES

1. Goodman MT, Wilkens LR, Hankin JH, et al. Association of soy and fiber consumption with the risk of endometrial cancer. *Am J Epidemiol.* 1997; 146:294–305.
2. Uckun FM, Messinger Y, Chen CL, et al. Treatment of therapy-refractory B-lineage acute lymphoblastic leukemia with an apoptosis-inducing CD19-directed tyrosine kinase inhibitor. *Clin Cancer Res.* 1999;5:3906–3913.
3. Kim H, Peterson TG, Barnes S. Mechanisms of action of the soy isoflavone genistein: emerging role for its effects via transforming growth factor β signaling pathways. *Am J Clin Nutr.* 1998;68(suppl):1418S–1425S.
4. Lamartiniere CA. Protection against breast cancer with genistein: a component of soy. *Am J Clin Nutri.* 2000;71:1705S–1707S.
5. Polkowski K, Mazurek AP. Biological properties of genistein. A review of in vitro and in vivo data. *Acta Pol Pharm.* 2000;57:135–155.
6. El-Zarruk AA, van den Berg HW. The anti-proliferative effects of tyrosine kinase inhibitors towards tamoxifen-sensitive and tamoxifen-resistant human breast cancer cell lines in relation to the epidermal growth factor receptors (EGF-R) and the inhibition of EGF-R tyrosine kinase. *Cancer Lett.* 1999;142:185–193.
7. Lian F, Bhuiyan M, Li YW, et al. Genistein-induced G_2-M arrest, $p21^{WAF1}$ upregulation, and apoptosis in a non-small-cell lung cancer cell line. *Nutr Cancer.* 1998;31:184–191.
8. Boros LG, Torday JS, Lim S, et al. Transforming growth factor β2 promotes glucose carbon incorporation into nucleic acid ribose through the nonoxidative pentose cycle in lung epithelial cells. *Cancer Res.* 2000;60: 1183–1185.
9. Peterson G. Evaluation of the biochemical targets of genistein in tumor cells. *J Nutr.* 1995;125:784S–789S.
10. Ju YH, Allred CD, Allred KF, et al. Physiological concentrations of dietary genistein dose-dependently stimulate growth of estrogen-dependent human breast cancer (MCF) tumors implanted in athymic nude mice. *J Nutr.* 2001;131:2957–2962.

11. Ju YH, Doerge DR, Allred KF, et al. Dietary genistein negates the inhibitory effect of tamoxifen on growth of estrogen-dependent human breast cancer (MCF-7) cells implanted in athymic mice. *Cancer Res.* 2002;62: 2474–2477.

12. Hughes TR, Marton MJ, Jones AR, et al. Functional discovery via a compendium of expression profiles. *Cell.* 2000;102:109–126.

13. Carpenter G, Wahl MI. The epidermal growth factor family. In: Sporn MB, Roberts AB, ed. *Peptide growth factors and their receptors 1.* New York: Springer-Verlag; 1990:69–171.

14. Nicholson S. Epidermal growth factor receptor (EGFr) status associated with failure of primary endocrine therapy in elderly postmenopausal patients with breast cancer. *Br J Cancer.* 1988;58:810–814.

15. Dalu A, Haskell JF, Coward L, et al. Genistein, a component of soy, inhibits the expression of the EGF and ErbB/Neu receptors in the rat dorsolateral prostate. *Prostate.* 1998;37:36–43.

16. Ruggeri BA, Huang L, Wood M, et al. Amplification and overexpression of the AKT2 oncogene in a subset of human pancreatic ductal adenocarcinomas. *Mol Carcinog.* 1998;21:81–86.

17. Yuan ZQ, Feldman RI, Sun M, et al. Inhibition of JNK by cellular stress- and tumor necrosis factor α-induced AKT2 through activation of the NF κB pathway in human epithelial cells. *J Biol Chem.* 2002;277:29973–29982.

18. Kaufmann K, Thiel G. Epidermal growth factor and thrombin induced proliferation of immortalized human keratinocytes is coupled to the synthesis of egr-1, a zinc finger transcriptional regulator. *J Cell Biochem.* 2002;85:381–391.

19. Kaufmann K, Thiel G. Epidermal growth factor and platelet-derived growth factor induce expression of egr-1, a zinc finger transcription factor, in human malignant glioma cells. *J Neurol Sci.* 2001;1889:83–91.

20. Eid MA, Kumar MV, Iczkowski KA, et al. Expression of early growth response genes in human prostate cancer. *Cancer Res.* 1998;58:2461–2468.

21. Liu JW, Lacy J, Sukhatme VP, et al. Granulocyte-macrophage colony-stimulating factor induces transcriptional activation of Egr-1 in murine peritoneal macrophages. *J Biol Chem.* 1991;266:5929–5933.

22. Kovary K, Bravo R. Existence of different Fos/Jun complexes during the G0-to-G1 transition and during exponential growth in mouse fibroblasts: differential role of Fos proteins. *Mol Cell Biol.* 1992;12:5015–5023.

23. Watanabe TK, Katagiri T, Suzuki M, et al. Cloning and characterization of two novel human cDNAs (NELL1 and NELL2) encoding proteins with six EGF-like repeats. *Genomics.* 1996;38:273–276.

24. Kuroda S, Oyasu M, Kawakami M, et al. Biochemical characterization and expression analysis of neural thrombospondin-1-like proteins NELL1 and NELL2. *Biochem Biophys Res Commun.* 1999;265:79–86.

25. Chen JK, Wang DW, Falck JR, et al. Transfection of an active cytochrome P450 arachidonic acid epoxygenase indicates that 14.15-epoxyeicosatrienoic acid functions as an intracellular second messenger in response to epidermal growth factor. *J Biol Chem.* 1999;274:4764–4769.

26. Kivisto KT, Kroemer HK, Eichelbaum M. The role of human cytochrome

27. Murray GI, Taylor MC, McFadyen MC, et al. Tumor-specific expression of cytochrome P450 CYP1B1. *Cancer Res.* 1997;57:3026–3031.

28. Markovits J, Linassier C, Fosse P, et al. Inhibitory effects of the tyrosine kinase inhibitor genistein on mammalian DNA topoisomerase II. *Cancer Res.* 1989;49:5111–5117.

29. Salti GI, Grewal S, Mehta RR, et al. Genistein induces apoptosis and topoisomerase II-mediated DNA breakage in colon cancer cells. *Eur J Cancer.* 2000;36:796–802.

30. Bordone L, Campbell C. DNA ligase III is degraded by calpain during cell death induced by DNA-damaging agents. *J Biol Chem.* 2002;277:26673–26680.

31. Zhu J, Tseng YH, Kantor JD, et al. Interaction of the Ras-related protein associated with diabetes Rad and the putative tumor metastasis suppressor NM23 provides a novel mechanism of GTPase regulation. *Proc Natl Acad Sci U S A.* 1999;96:14911–14918.

32. Moyers JS, Bilan PJ, Reynet C, et al. Overexpression of Rad inhibits glucose uptake in cultured muscle and fat cells. *J Bio Chem.* 1996;271: 23111–23116.

33. Boros LG, Bassilian S, Lim S, et al. Genistein inhibits nonoxidative ribose synthesis in MIA pancreatic adenocarcinoma cells: a new mechanism of controlling tumor growth. *Pancreas.* 2001;22:1–7.

34. Boros LG, Lapis K, Szende B. Wheat germ extract decrease glucose uptake and RNA ribose formation but increase fatty acid synthesis in MIA pancreatic adenocarcinoma cells. *Pancreas.* 2001;23:141–147.

35. Falvella FS, Pascale RM, Gariboldi M, et al. Stearoyl-Coa desaturase 1 (Scd1) gene overexpression is associated with genetic predisposition to hepatocarcinogenesis in mice and rats. *Carcinogenesis.* 2002;23:1933–1936.

36. Lu J, Pei H, Kaeck M, et al. Gene expression changes associated with chemically induced rat mammary carcinogenesis. *Mol Carcinog.* 1997; 20:204–215.

37. Chajes V, Hulten K, Van Kappel AL, et al. Fatty-acid composition in serum phospholipids and risk of breast cancer: an incident case-control study in Sweden. *Int J Cancer.* 1999;83:585–590.

38. Adlercreutz H, Mazur W. Phyto-oestrogens and Western diseases. *Ann Med.* 1997;29:95–120.

39. Barnes S. Evolution of the health benefits of soy isoflavones. *Proc Soc Exp Med.* 1998;217:386–392.

40. Xie KP. Interleukin-8 and human cancer biology. *Cytokine Growth Factor Rev.* 2001;12:375–391.

41. Yoshida S, Ono M, Shono T, et al. Involvement of interleukin-8, vascular endothelial growth factor, and basic fibroblast growth factor in tumor necrosis factor alpha-dependent angiogenesis. *Mol Cell Biol.* 1997;17: 4015–4023.

42. Helferich WG. Paradoxical effects of the soy phytoestrogen genistein on growth of human breast cancer cells in vitro and in vivo. *Am J Clin Nutr.* 1998;68:1524S–1525S.

P450 enzymes in the metabolism of anticancer agents: implications for drug interactions. *Br J Clin Pharmacol.* 1995;40:523–530.

Reprogramming of human postmitotic neutrophils into macrophages by growth factors

Hiroto Araki, Naoyuki Katayama, Yoshihiro Yamashita, Hiroyuki Mano, Atsushi Fujieda, Eiji Usui, Hidetsugu Mitani, Kohshi Ohishi, Kazuhiro Nishii, Masahiro Masuya, Nobuyuki Minami, Tsutomu Nobori, and Hiroshi Shiku

It is generally recognized that postmitotic neutrophils give rise to polymorphonuclear neutrophils alone. We obtained evidence for a lineage switch of human postmitotic neutrophils into macrophages in culture. When the CD15+CD14− cell population, which predominantly consists of band neutrophils, was cultured with granulocyte macrophage–colony-stimulating factor, tumor necrosis factor-α, interferon-γ, and interleukin-4, and subsequently with macrophage colony-stimulating factor alone, the resultant cells had morphologic, cytochemical, and phenotypic features of macrophages. In contrast to the starting population, they were negative for myeloperoxidase, specific esterase, and lactoferrin, and they upregulated nonspecific esterase activity and the expression of macrophage colony-stimulating factor receptor, mannose receptor, and HLA-DR. CD15+CD14− cells proceeded to macrophages through the CD15−CD14− cell population. Microarray analysis of gene expression also disclosed the lineage conversion from neutrophils to macrophages. Macrophages derived from CD15+CD14− neutrophils had phagocytic function. Data obtained using 3 different techniques, including Ki-67 staining, bromodeoxyuridine incorporation, and cytoplasmic dye labeling, together with the yield of cells, indicated that the generation of macrophages from CD15+CD14− neutrophils did not result from a contamination of progenitors for macrophages. Our data show that in response to cytokines, postmitotic neutrophils can become macrophages. This may represent another differentiation pathway toward macrophages in human postnatal hematopoiesis. (Blood. 2004;103:2973-2980)

© 2004 by The American Society of Hematology

Introduction

One apparent characteristic of the hematopoietic system is that all types of mature cells with distinct functions are continuously replaced by cells derived from hematopoietic stem cells that reside mainly in the bone marrow and have the ability for self-renewal and multilineage differentiation.[1,2] In the process of differentiation, hematopoietic stem cells sequentially lose multilineage potential and generate lineage-committed progenitors with limited developmental capacity. Lineage-committed progenitors give rise to precursors that eventually differentiate into mature blood cells. After commitment to specific lineages, hematopoietic progenitor cells are incapable of producing mature cells of other lineages. For example, neutrophilic monopotent progenitors proliferate and differentiate into neutrophils, and progenitors restricted to a macrophage lineage cannot give rise to mature cells other than macrophages.

Several studies have focused on a lineage switch in the hematopoietic differentiation pathway. Boyd and Schrader[3] reported that murine pre–B-cell lines differentiate into macrophage-like cells in response to the demethylating drug, 5-azacytidine. B-lineage cells have been also shown to transit into neutrophils or natural killer (NK)/T-lineage cells.[4-8] Furthermore, the macrophage cell line differentiates into B-lineage cells.[9] Common lymphoid progenitors that exogenously express cytokine receptors or transcriptional factors develop myeloid lineage cells.[10-12] In addition to

these lineage switches, lineage conversions within myeloid lineages have also been observed in experiments using cell lines and transformed cells. Enforced expression of transcriptional factors such as GATA-1 and PU.1 leads to the lineage switch of myeloid cells to cells with another myeloid phenotype.[12-17] These lineage switches include myeloid to megakaryocytic, myeloid to eosinophilic, myeloid to erythroid, and erythroid to myeloid conversions. The ectopic expression of PU.1 and C/EBP also results in the commitment of hematopoietic progenitors to an eosinophilic lineage.[18-20] With respect to normal primary cells, it has been reported that murine B-cell precursor cells acquire the potential to differentiate into macrophage-like cells when they are transferred to myeloid culture conditions.[21] Normal murine early T progenitor cells also generate macrophages in cultures supplemented with conditioned medium from a thymic stromal cell line or in the presence of cytokines.[22] Thus, normal murine lymphoid progenitors may retain the potential to differentiate into macrophages. Reynaud et al[23] reported that human cord blood–derived pro-B cells with DJ$_H$ rearrangements of the immunoglobulin (Ig) locus generate macrophages, NK cells, and T cells. However, it is unknown whether the lineage switch occurs in normal human mature hematopoietic cells.

We conducted research to determine whether normal postmitotic neutrophils are able to differentiate into other types of mature

cells. We found that human postmitotic neutrophils switched their differentiation program and acquired the features of macrophages in cultures supplemented with cytokines. These data support the possibility that postmitotic neutrophils commonly thought to be restricted to the neutrophilic differentiation pathway can become macrophages, and we argue that the lineage switch of human mature blood cells may, at least in part, be relevant to normal hematopoietic differentiation.

Materials and methods

Cytokines

Recombinant human macrophage colony-stimulating factor (M-CSF) and interferon-γ (IFN-γ) were purchased from R&D Systems (Minneapolis, MN). Recombinant human granulocyte macrophage–colony-stimulating factor (GM-CSF) was provided by Kirin Brewery (Tokyo, Japan). Recombinant human tumor necrosis factor-α (TNF-α) was a gift from Dainippon Pharmaceutical (Suita, Japan). Recombinant human interleukin-4 (IL-4) was provided by Ono Pharmaceutical (Osaka, Japan). Cytokines were used at the following concentrations: M-CSF, 100 ng/mL; IFN-γ, 25 IU/mL; GM-CSF, 10 ng/mL; TNF-α, 20 ng/mL; and IL-4, 10 ng/mL.

Cell preparation

Peripheral blood was obtained from healthy Japanese donors given subcutaneous injections of granulocyte colony-stimulating factor (G-CSF) to harvest peripheral blood stem cells. Each donor gave written, informed consent. Peripheral blood mononuclear cells (PBMCs) were separated by centrifugation on Ficoll-Hypaque, washed with Ca^{2+}-, Mg^{2+}-free phosphate-buffered saline (PBS), and suspended in PBS with 0.1% bovine serum albumin (BSA) (Sigma Chemical, St Louis, MO). $CD15^+CD14^-$ cells were separated from PBMCs using CD14 and CD15 immunomagnetic beads (MACS; Miltenyi Biotec, Auburn, CA), according to the manufacturer's instructions. $CD14^+$ and $CD8^+$ cells were also separated from PBMCs using CD14 and CD8 immunomagnetic beads (MACS; Miltenyi Biotec), respectively. Healthy donors gave written, informed consent. The purity of $CD15^+CD14^-$, $CD14^+$, or $CD8^+$ cells exceeded 99%.

Culture

Culture medium was RPMI 1640 (Nissui Pharmaceutical, Tokyo, Japan) supplemented with 2 mM L-glutamine, 50 U/mL penicillin, 50 μg/mL streptomycin, and 10% fetal bovine serum (FBS) (HyClone Laboratories, Logan, UT). $CD15^+CD14^-$ cells (1 × 10^6/mL) were cultured with designated combinations of cytokines in a 24-well tissue culture plate (Nunc, Roskilde, Denmark) for 18 days. Half of the culture medium was replaced with fresh medium containing cytokines every 3 to 4 days. In some experiments, cells were plated with designated combinations of cytokines; on day 11 of culture, the cells were washed 3 times with PBS and replated in cultures containing M-CSF. $CD14^+$ and $CD15^+CD14^-$ cells (1 × 10^6/mL) were cultured in the presence of M-CSF for 7 days. Viable cells were counted using trypan blue dye exclusion methods.

Morphologic cell analysis

Cytospin preparations of freshly isolated and cultured cells were stained with May-Grünwald-Giemsa solution, myeloperoxidase (MPO) staining kit, and double-specific (naphthol AS-D chloroacetate esterase)/nonspecific (α-naphthyl butyrate esterase) esterase staining kit.

Cell cycle analysis

Cell cycle analysis was made using the CycleTEST PLUS DNA Reagent Kit (Becton Dickinson, San Jose, CA) according to the manufacturer's instructions. Nuclear DNA content of freshly isolated $CD15^+CD14^-$ cells was analyzed on a FACSCalibur flow cytometer (Becton Dickinson) with ModFit software (Verity Software House, Topsham, ME). HPB-NULL cells

(American Type Culture Collection, Manassas, VA) were used as a control. HPB-NULL cells were passaged every 24 hours for 3 days before use to minimize differences among experimental conditions.

Flow cytometric analysis

The following murine or rat monoclonal antibodies (mAbs) were used: anti–CD14-phycoerythrin (anti–CD14-PE), anti–CD15-fluorescein isothiocyanate (anti–CD15-FITC), and anti–HLA-DR-PE (Becton Dickinson); anti–MPO-FITC (DAKO, Glostrup, Denmark); anti–lactoferrin-PE (Immunotech, Marseille, France); anti–c-fms/M-CSF receptor (anti–c-fms/M-CSFR) (Oncogene Research, Boston, MA); anti–mannose receptor-PE, anti–Ki-67-FITC, which reacts with a proliferation-associated nuclear antigen, antibromodeoxyuridine (anti-BrdU)–FITC, and anti–rat IgG2b-FITC (Becton Dickinson PharMingen, San Diego, CA). Rat immunoglobulin and FITC- or PE-labeled mouse immunoglobulin served as isotype control: rat IgG2b and mouse IgM-FITC (Becton Dickinson PharMingen); mouse IgG1-FITC, IgG1-PE, and IgG2a-PE (Becton Dickinson); and mouse IgG2b-PE (Coulter, Miami, FL).

For membrane staining, cells were incubated with mAbs for 30 minutes on ice and washed 3 times with PBS. Intracellular molecules were stained, using Cytofix/Cytoperm Kit (PharMingen, San Diego, CA). Cells were fixed for 20 minutes at 4°C with formaldehyde-based fixation medium, washed, resuspended in permeabilization buffer containing sodium azide and saponin, and stained with mAbs for 30 minutes at 4°C. Cells were washed with the permeabilization buffer and PBS. HPB-NULL cells were used as a positive control for Ki-67 staining. Flow cytometric analysis was performed, using a FACSCalibur flow cytometer. CellQuest software (Becton Dickinson) was used for data acquisition and analysis.

BrdU and carboxyfluorescein diacetate succinimidyl ester (CFSE) labeling

For BrdU pulse labeling, freshly isolated and cultured cells (1 × 10^6/mL) were incubated with 5 μg/mL BrdU (Sigma Chemical) for 40 minutes. The cells were washed with 0.1% BSA PBS, fixed with ice-cold 70% ethanol for 30 minutes at −20°C, and treated with 4 N HCl/0.5% Tween-20 at room temperature for 20 minutes for DNA denaturation. Acid was neutralized with 0.1 M $Na_2B_4O_7$. After washing with 0.1% BSA PBS, the cells were stained with FITC-conjugated anti-BrdU mAb. BrdU incorporation was analyzed using a FACSCalibur cytometer.[24] HPB-NULL cells served as a positive control for BrdU labeling.

Freshly isolated $CD15^+CD14^-$ cells (1 × 10^6/mL) were labeled for 10 minutes at 37°C with 0.5 μM CFSE (Lambda, Graz, Austria) PBS, a cytoplasmic dye that is equally diluted between daughter cells, and were washed 3 times with 10% FBS RPMI 1640. CFSE-labeled $CD15^+CD14^-$ cells were cultured as described above. $CD8^+$ cells (1 × 10^6/mL) were labeled with CFSE, washed with 10% FBS RPMI 1640, and cultured with T-cell expander beads (CD3/CD28 T-cell expander; DynalBiotech, Oslo, Norway) at a 1:3 bead-to-cell ratio for 5 days. CFSE-labeled freshly isolated and cultured cells were analyzed for fluorescence intensity using a FACSCalibur cytometer.[25]

Microarray

Microarray assay was carried out as described.[26,27] Total RNA extracted from freshly isolated and cultured cells by the acid guanidinium method was used to synthesize double-stranded cDNA. Biotin-labeled cRNA was prepared from each cDNA by ENZO BioArray High-Yield RNA Transcript Labeling kit (Affymetrix, Santa Clara, CA), and hybridized with a GeneChip HGU133A microarray (Affymetrix) harboring more than 22 000 human probe sets. Hybridization, washing, and detection of signals on the arrays were performed using the GeneChip system (Affymetrix) according to the manufacturer's protocols. Fluorescence intensity for each gene was normalized on the basis of the median expression value of the positive control genes (Affymetrix; HGU133Anorm.MSK) in each hybridization. Every microarray analysis was repeated twice. Hierarchical clustering and Welch analysis of variance (ANOVA) of the data set were conducted by using GeneSpring 6.0 software (Silicon Genetics, Redwood, CA).

Phagocytosis

Cultured cells (2×10^5/mL) were incubated with FITC-dextran (40 000 molecular weight; Sigma Chemical) or FITC-latex beads (2 μm; Polysciences, Warrington, PA) for 1 hour at 37°C or 4°C. The uptake of FITC-dextran and FITC-latex beads was halted by the addition of cold 1% FBS PBS. After washing 3 times with 1% FBS PBS, cells were analyzed on a FACS flow cytometer.[28,29]

Results

CD15$^+$CD14$^-$ neutrophils generate macrophages

We isolated CD15$^+$CD14$^-$ cells from human blood samples. Portions of May-Grünwald-Giemsa–, MPO-, and double-specific/nonspecific esterase–stained preparations are presented in Figure 1A. The CD15$^+$CD14$^-$ cell fraction consisted of myelocytes, metamyelocytes, band cells, and segmented cells. Proportions of myelocytes, metamyelocytes, band cells, and segmented cells were 0.6% ± 0.2%, 9.2% ± 2.5%, 87.6% ± 2.5%, and 2.6% ± 0.4%, respectively (n = 5). CD15$^+$CD14$^-$ cells were positive for MPO and specific esterase but negative for nonspecific esterase. These staining patterns were found in all portions of cytospin preparations. We analyzed the cell cycle characteristics of CD15$^+$CD14$^-$ cells. All CD15$^+$CD14$^-$ cells were found in G$_1$ phase of the cell cycle (Figure 1B), supporting the notion that these cells are postmitotic. The expression of MPO, M-CSFR, lactoferrin, mannose receptor, and HLA-DR was assessed by phenotypic analysis (Figure 1C). CD15$^+$CD14$^-$ cells were MPO$^+$, M-CSFR$^-$, lactoferrin$^+$, mannose receptor$^-$, and HLA-DR$^-$, a finding compatible with typical features of mature neutrophils. CD14$^+$ cells were also prepared from blood samples. Cultures of CD14$^+$ cells in the presence of M-CSF gave rise to cells with small nuclei and intracytoplasmic vacuoles. These
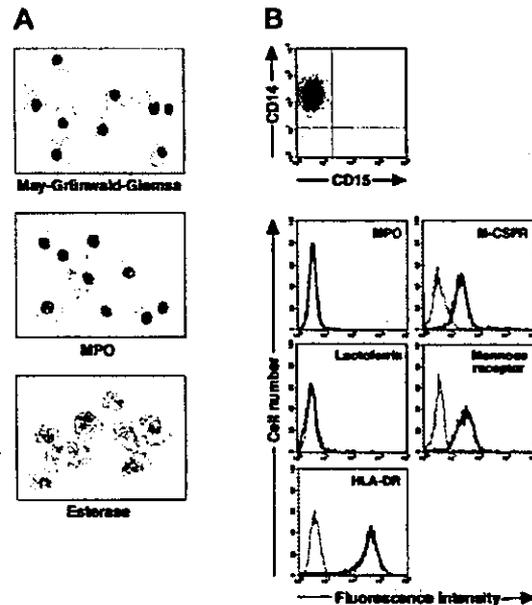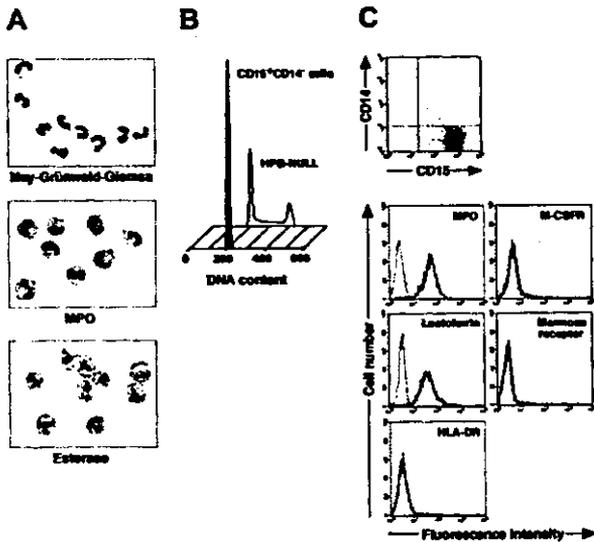

Figure 1. Cytochemistry and phenotype of freshly isolated CD15$^+$CD14$^-$ cells. (A) Photographs of May-Grünwald-Giemsa–, MPO-, and double-specific/nonspecific esterase–stained cytospin preparations; original magnification, × 400. (B) Nuclear DNA analysis of CD15$^+$CD14$^-$ cells was performed using a FACSCalibur flow cytometer. HPB-NULL cells were used as controls. Cell cycle distribution of HPB-NULL cells was as follows: with G$_1$ phase, 42.9%; S phase, 30.5%; and G$_2$/M phase, 26.6%. (C) The expression of CD15/CD14, MPO, M-CSFR, lactoferrin, mannose receptor, and HLA-DR was analyzed using a FACSCalibur flow cytometer. In the histograms, the thick and thin lines show the expression of the indicated molecules and isotype controls, respectively. Representative data from 5 independent experiments are shown.
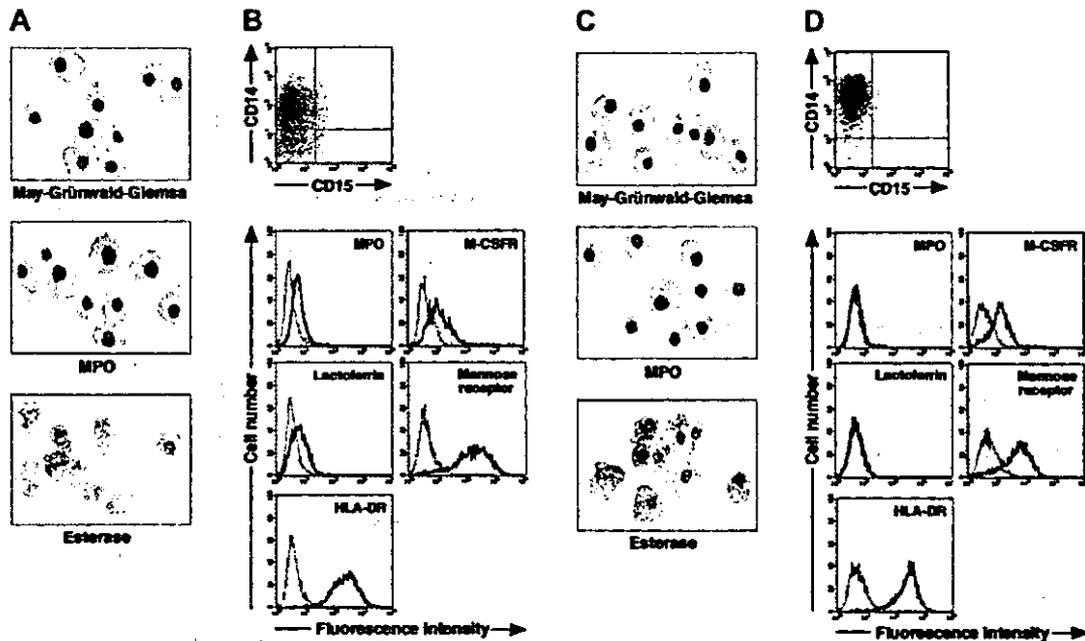

Figure 2. Cytochemistry and phenotype of cells obtained from 7-day culture of freshly isolated CD14$^+$ cells with M-CSF. (A) Photographs of May-Grünwald-Giemsa–, MPO-, and double specific/nonspecific esterase–stained cytospin preparations; original magnification, × 400. (B) The expression of CD15/CD14, MPO, M-CSFR, lactoferrin, mannose receptor, and HLA-DR was analyzed using a FACSCalibur flow cytometer. In the histograms, the thick and thin lines show the expression of the indicated molecules and isotype controls, respectively. Yield of cultured cells was 52.8% ± 9.8% (n = 5). Representative data from 5 independent experiments are shown.

cells showed nonspecific esterase activity but not MPO or specific esterase activity (Figure 2A), and they exhibited the phenotype of CD15$^-$ CD14$^+$, MPO$^-$, M-CSFR $^+$, lactoferrin$^-$, mannose receptor$^+$, and HLA-DR$^+$ (Figure 2B), which suggested that the resultant cells were macrophages. CD15$^+$CD14$^-$ cells were also cultured in the presence of M-CSF for 7 days. The yield was less than 2% of the starting population. Surviving cells retained the features of neutrophils (data not shown).

To determine whether postmitotic neutrophils have the potential to alter the lineage, we attempted to drive CD15$^+$CD14$^-$ cells to become cells of a monocyte/macrophage lineage, using cultures supplemented with cytokines. The combination of GM-CSF, M-CSF, TNF-α, and IFN-γ was chosen because GM-CSF, M-CSF, TNF-α, and IFN-γ are known to favor the differentiation of monocytes and their progenitors into macrophages.[1,30-36] Because M-CSF is a cytokine specific for, and late-acting in, a monocyte/macrophage lineage, we cultured CD15$^+$CD14$^-$ cells in the presence of GM-CSF, TNF-α, and IFN-γ for 11 days and subsequently replated the cells in cultures with M-CSF alone. On day 18 after the initiation of culture, cultured cells were harvested and characterized in morphologic, cytochemical, and phenotypic analyses. These cells had macrophage morphology (Figure 3A). Their MPO or specific esterase activity was not detected using light microscopy; however, the nonspecific esterase reaction was positive. CD14 expression was induced in a substantial, although not the entire, population of the resultant cells, but CD15 expression was completely lost (Figure 3B). When compared with freshly isolated CD15$^+$CD14$^-$ cells, the resultant cells did not entirely down-regulate MPO and lactoferrin yet they considerably up-regulated M-CSFR, mannose receptor, and HLA-DR. This culture condition yielded 1.8% ± 0.6% (n = 5) of the starting CD15$^+$CD14$^-$ cell population. These data suggest that GM-CSF, TNF-α, IFN-γ, and M-CSF allow CD15$^+$CD14$^-$ cells to become macrophages.

Figure 3. Cytochemistry and phenotype of cells obtained from culture of freshly isolated CD15⁺CD14⁻ neutrophils. (A-B) Freshly isolated CD15⁺CD14⁻ neutrophils were cultured with GM-CSF, TNF-α, and IFN-γ for 11 days, followed by additional 7-day culture with M-CSF alone. (C-D) Freshly isolated CD15⁺CD14⁻ neutrophils were cultured with GM-CSF, TNF-α, IFN-γ, and IL-4 for 11 days, followed by additional 7-day culture with M-CSF alone. (A,C) Photographs of May-Grünwald-Giemsa-, MPO-, and double specific/nonspecific esterase–stained cytospin preparations; original magnification, × 400. (B,D) The expression of CD15/CD14, MPO, M-CSFR, lactoferrin, mannose receptor, and HLA-DR was analyzed using a FACSCalibur flow cytometer. In the histograms, the thick and thin lines show the expression of the indicated molecules and isotype controls, respectively. Representative data from 5 independent experiments are shown.

Next, we searched for cytokine(s). The addition of cytokines to cultures would allow cells derived from CD15⁺CD14⁻ cells to acquire features more typical of macrophages. After testing several cytokines, we found that the appropriate conditions could be satisfied by supplementation with IL-4. When cultured with GM-CSF, TNF-α, IFN-γ, and IL-4 for 11 days and with M-CSF alone for 7 days, CD15⁺CD14⁻ cells gave rise to cells with morphologic characteristics of macrophages. The resultant cells were negative for MPO and specific esterase activities and positive for nonspecific esterase activity on cytospin preparations (Figure 3C). Phenotypic analysis showed that the resultant cells lacked CD15 and exclusively expressed CD14. MPO and lactoferrin were completely down-regulated, whereas the high levels of M-CSFR, mannose receptor, and HLA-DR expression were retained (Figure 3D), as in the macrophage phenotype induced from CD14⁺ cells by M-CSF. Strikingly, the yield increased to 15.1% ± 3.6% (n = 5) of the starting CD15⁺CD14⁻ cell population. These observations unambiguously demonstrated a cytokine-induced lineage switch of postmitotic neutrophils to macrophages. We also cultured CD15⁺CD14⁻ cells in the presence of GM-CSF, TNF-α, IFN-γ, and IL-4 for 11 days and analyzed their phenotypes using flow cytometry. Cultured cells expressed neither CD15 nor CD14 (Figure 4A). MPO and lactoferrin were detected at low levels, whereas the expression levels of M-CSFR, mannose receptor, and HLA-DR were high (Figure 4B). These data suggest that the expression levels of molecules that characterize postmitotic neutrophils or macrophages are not simultaneously altered during this lineage switch program.

Gene expression profiles of CD15⁺CD14⁻ neutrophils and macrophages

Given that the combination of cytokines consisting of GM-CSF, TNF-α, IFN-γ, IL-4, and M-CSF allowed for the generation of macrophages from CD15⁺CD14⁻ neutrophils, as determined by morphologic, cytochemical, and phenotypic analyses, we com-

pared the gene expression profiles of freshly isolated CD15⁺CD14⁻ neutrophils, CD15⁺CD14⁻ neutrophil–derived macrophages, and CD14⁺ cell–derived macrophages using high-density oligonucleotide microarrays. Because every microarray was repeated twice, the mean expression intensity was calculated for each gene and was used for the following analysis. Among our expression data set, first searched were the genes expressed abundantly in CD15⁺CD14⁻ neutrophils but not in CD14⁺ cell–derived macrophages. Table 1 shows 10 such genes that had an expression level of more than 100 arbitrary units in CD15⁺CD14⁻ neutrophils and the highest ratio of the expression level between CD15⁺CD14⁻ neutrophils and CD14⁺

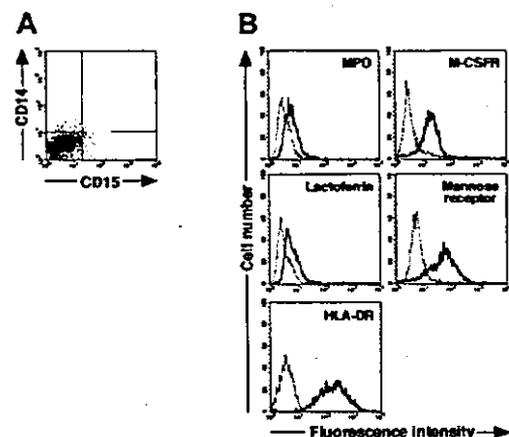**Figure 4. Cytochemistry and phenotype of cells obtained from culture of freshly isolated CD15⁺CD14⁻ neutrophils with GM-CSF, TNF-α, IFN-γ, and IL-4 for 11 days.** (A) Expression pattern of CD15/CD14. (B) The expression of CD15/CD14, MPO, lactoferrin, M-CSFR, mannose receptor, and HLA-DR was analyzed using a FACSCalibur flow cytometer. In the histograms, the thick and thin lines show the expression of the indicated molecules and isotype controls, respectively. Representative data from 5 independent experiments are shown.

Table 1. Genes specifically expressed in CD15⁺CD14⁻ neutrophils

Gene symbol	GenBank accession no.	CD15⁺CD14⁻ neutrophil/ CD14⁺ cell-derived macrophage ratio	CD15⁺CD14⁻ neutrophils	CD14⁺ cell-derived macrophages	CD15⁺CD14⁻ neutrophil-derived macrophages
bA209J19.1	AL390736	5412.83	1623.85	0.30	0.60
LTF	NM_002343	2795.52	3773.95	1.35	1.50
DEFA3	NM_004084	1142.16	15 761.80	13.80	9.65
S100P	NM_005980	1099.67	3189.05	2.90	28.05
SGP28	NM_006061	699.78	314.90	0.45	0.45
CEACAM8	M33326	588.24	1323.55	2.25	3.30
LCN2	NM_005564	550.64	2945.90	5.35	8.90
DEFA4	NM_001925	499.83	2849.05	5.70	3.85
CD24	BG327863	474.81	759.70	1.60	8.75
FIZZ3	NM_020415	452.96	1223.00	2.70	5.90

Mean expression levels of genes in CD15⁺CD14⁻ neutrophils, CD14⁺ cell-derived macrophages, and CD15⁺CD14⁻ neutrophil-derived macrophages are shown in arbitrary units. The ratio between the first 2 is indicated in the CD15⁻CD14⁻ neutrophil/CD14⁺ cell-derived macrophage ratio.

cell–derived macrophages. Interestingly, all these CD15⁺CD14⁻ neutrophil-specific genes were also transcriptionally silent in CD15⁺CD14⁻ neutrophil-derived macrophages, as in CD14⁺ cell-derived macrophages. A well-known marker for granulocytes, CD24 (GenBank accession number AA761181) was only expressed in CD15⁺CD14⁻ neutrophils but not in CD15⁺CD14⁻ neutrophil-derived macrophages or CD14⁺ cell-derived macrophages. Conversely, we also tried to extract CD14⁺ cell-derived, macrophage-specific genes by comparing CD14⁺ cell-derived macrophages and CD15⁺CD14⁻ neutrophils (Table 2). Again, expression levels of these genes in the CD15⁺CD14⁻ neutrophil-derived macrophages were highly similar to those in CD14⁺ cell-derived macrophages. A monocyte/macrophage-specific cell surface antigen, CD163 (Z22969), was abundantly expressed in the CD15⁺CD14⁻ neutrophil-derived macrophages and the CD14⁺ cell-derived macrophages, but not in the CD15⁺CD14⁻ neutrophils. Hierarchical clustering analysis of these lineage-specific genes showed the similarity between gene expression profiles of CD15⁺CD14⁻ neutrophil-derived macrophages and CD14⁺ cell-derived macrophages (Figure 5A). Next, to statistically examine this similarity, we directly compared the 4 expression data sets of CD15⁺CD14⁻ neutrophils (n = 2) and CD14⁺ cell-derived macrophages (n = 2) and attempted to identify the genes, whose expression was different in the 2 groups (Welch ANOVA, $P < .001$). The expression profiles of such 9 lineage-dependent genes (Table 3) were then used to measure the similarity between CD14⁺ cell-derived macrophages and the other 2 groups. As shown in Figure 5B, 2-way clustering analysis[37] of 6 data sets (3 groups) clearly indicated that, with regard to gene expression profile, CD15⁺CD14⁻ neutrophil-derived macrophages were similar to

CD14⁺ cell–derived macrophages, separated from CD15⁺CD14⁻ neutrophils.

Phagocytic activity of CD15⁺CD14⁻ neutrophil-derived macrophages

Morphology, cytochemistry, phenotype, and gene expression of cultured cells in the presence of GM-CSF, TNF-α, IFN-γ, IL-4, and M-CSF indicated that CD15⁺CD14⁻ neutrophils became macrophages. Therefore, we next evaluated the phagocytic activity of these macrophages using FITC-dextran and FITC-latex beads. The potential for CD15⁺CD14⁻ neutrophil-derived macrophages to incorporate dextran and latex beads was comparable to that of CD14⁺ cell–derived macrophages (Figure 6).

Proliferative characteristics during culture

It is possible that macrophages induced from CD15⁺CD14⁻ neutrophils were derived from a small number of hematopoietic progenitor cells for macrophages that contaminated the CD15⁺CD14⁻ cell population and consequently proliferated. To exclude this possibility, we analyzed proliferative characteristics of the cultured cells; representative data are presented in Figure 7. In Figure 7A, the yield of cultured cells was 15.1%, on day 18 of culture. Reactivity with Ki-67 and incorporation of BrdU were tested on the indicated days of culture.[24,38] Ki-67⁺ or BrdU⁺ cells were not evident throughout the culture. Ki-67 expression and BrdU incorporation were observed most and approximately 30%, respectively, of HPB-NULL cells, which served as positive controls. We also used the carboxyfluorescein diacetate succinimidyl ester

Table 2. Genes specifically expressed in CD14⁺ cell-derived macrophages

Gene symbol	GenBank accession no.	CD14⁺ cell-derived macrophage/CD15⁺CD14⁻ neutrophil ratio	CD14⁺ cell-derived macrophages	CD15⁺CD14⁻ neutrophils	CD15⁺CD14⁻ neutrophil-derived macrophages
SEPP1	NM_005410	643.60	1769.90	2.75	1373.45
DAB2	NM_001343	307.52	1183.95	3.85	513.20
CD163	Z22969	256.43	2602.75	10.15	1034.35
ME1	NM_002395	197.02	551.65	2.80	310.10
CCL2	S69738	196.38	1708.50	8.70	351.10
ATP1B1	BC000006	180.35	775.50	4.30	408.85
FN1	BC005858	169.67	972.70	5.75	155.60
FN1	AK026737	162.44	1210.15	7.45	191.65
TGFBI	NM_000358	131.99	4045.55	30.65	3030.45
PMP22	L03203	129.14	1091.25	8.45	59.20

Mean expression levels of the genes in CD14⁺ cell-derived macrophages, CD15⁺CD14⁻ neutrophils, and CD15⁻CD14⁻ neutrophil-derived macrophages are shown in arbitrary units. The ratio between the first 2 is indicated in the CD14⁺ cell-derived macrophage/CD15⁺CD14⁻ neutrophil ratio.
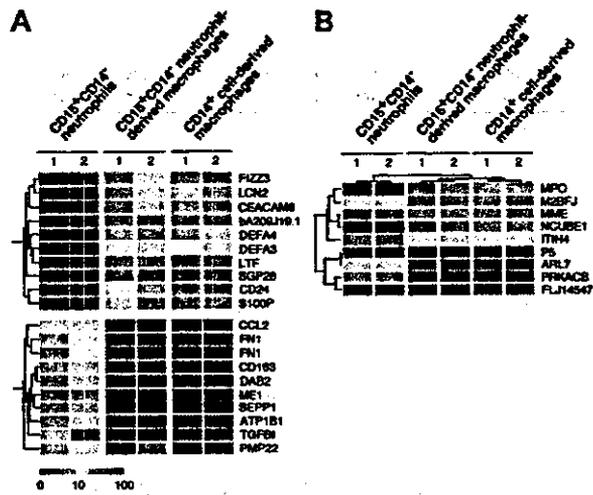
Figure 5. Expression profiles of neutrophil- and macrophage-specific genes. (A) Hierarchical clustering based on the expression intensities in CD15⁺CD14⁻ neutrophils, CD15⁺CD14⁻ neutrophil-derived macrophages, and CD14⁺ cell-derived macrophages was conducted for 10 genes with a specific expression in CD15⁺CD14⁻ neutrophils and CD14⁺ cell-derived macrophages (top panel) or in CD14⁺ cell-derived macrophages (bottom panel). Each row represents a single gene on the microarray, and each column represents a separate sample. Expression intensity of each gene is shown color coded, according to the scale at the bottom, and the gene symbols are indicated on the right. Expression data of these genes are available on request. (B) The gene tree was constructed using 2-way clustering analysis of the genes that are differentially (Welch ANOVA, P < .001) expressed between CD15⁺CD14⁻ neutrophils and CD14⁺ cell-derived macrophages. Each row represents a single gene on the microarray, and each column represents a separate sample. Expression intensity of each gene is shown color coded, according to the scale in panel A.

(CFSE) labeling technique to confirm that CD15⁺CD14⁻ neutrophils passed through no cell division during culture.²⁵ Analysis of the CFSE labeling pattern in CD8⁺ T cells, which had elicited several rounds of the cell cycle in response to CD3/CD28 T-cell expander beads, displayed a number of peaks of fluorescence (Figure 7B). However, the CFSE fluorescence remained a single peak in the cells generated by culturing CD15⁺CD14⁻ neutrophils with GM-CSF, TNF-α, IFN-γ, and IL-4 and subsequently with M-CSF alone. These data indicate that the generation of macrophages from the CD15⁺CD14⁻ cell population in culture is not associated with cell division.

Discussion

Lineage switch of normal primary cells has been noted in murine lymphoid progenitor cells.²¹,²² Montecino-Rodriguez et al²¹ ob-

Table 3. Genes with statistically different expression between CD15⁺CD14⁻ neutrophils and CD14⁺ cell-derived macrophages

Gene symbol	GenBank accession no.
MPO	J02694
H2BFJ	NM_003524
MME	NM_007287
NCUBE1	AF151039
ITIH4	D38535
P5	BC001312
ARL7	NM_005737
PRKACB	AA130247
FLJ14517	AV7113053

Gene symbols and GenBank accession numbers are shown for genes that exhibited significant differences in expression level between the 2 groups (Welch ANOVA, P < .001).
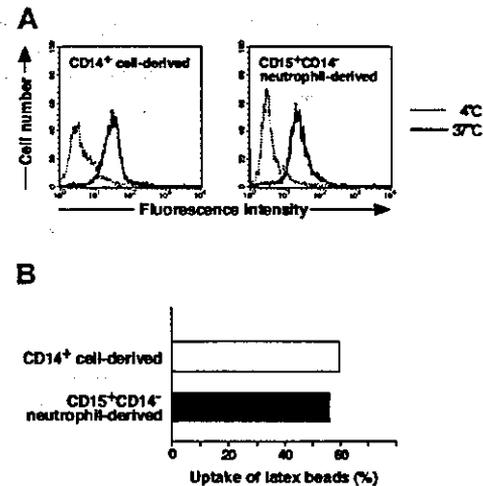

Figure 6. Phagocytic assay of CD15⁺CD14⁻ neutrophil-derived macrophages with FITC-dextran and FITC-latex beads. (A) CD15⁺CD14⁻ neutrophil- and CD14⁺ cell-derived macrophages were incubated with FITC-dextran for 1 hour at 37°C or 4°C, washed with cold PBS supplemented with 1% FBS, and analyzed using a FACSCalibur flow cytometer. Data are presented using histograms. (B) CD15⁺CD14⁻ neutrophil- and CD14⁺ cell-derived macrophages were incubated with FITC-latex beads for 1 hour at 37°C or 4°C, washed with cold PBS supplemented with 1% FBS, and analyzed with a FACSCalibur flow cytometer. Data are expressed as percentage of positive cells. Experiments were repeated 5 times with identical results.

served that a subpopulation of B-cell precursors in the bone marrow gave rise not only to B cells but also to macrophages in cultures supplemented with IL-3, IL-6, c-kit ligand, and GM-CSF. Lee et al²² demonstrated that fetal thymocytes differentiate into
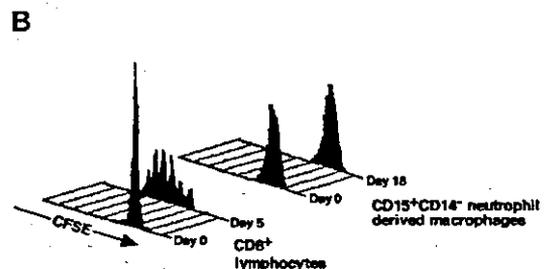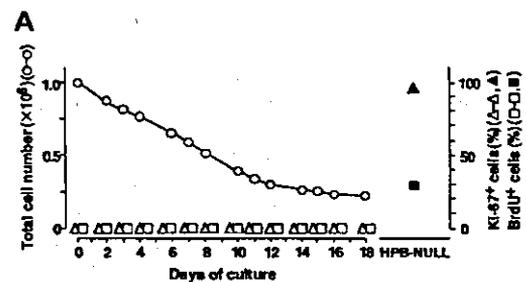

Figure 7. Analysis of proliferation profile. (A) CD15⁺CD14⁻ neutrophils were cultured with GM-CSF, TNF-α, IFN-γ, and IL-4 for 11 days, washed, and recultured with M-CSF alone for an additional 7 days. CD15⁺CD14⁻ neutrophils and the cultured cells were tested for Ki-67 staining and BrdU incorporation. Ki-67⁺ and BrdU⁺ cells were counted using a FACSCalibur flow cytometer, and the numbers were expressed as percentages. HPB-NULL cells were used as positive controls. Numbers of cultured cells are also indicated. Representative data from 5 independent experiments are shown. (B) CD15⁺CD14⁻ neutrophils were cultured with GM-CSF, TNF-α, IFN-γ, and IL-4 for 11 days, washed, and recultured with M-CSF alone for another 7 days. CD15⁻CD14⁻ neutrophils and the cultured cells were incubated with CFSE. Cell division patterns were analyzed using a FACSCalibur flow cytometer. CD8⁺ cells that underwent several rounds of the cell cycle in response to CD3/CD28 beads were used as positive controls. Experiments were repeated 5 times with identical results.

macrophages in the presence of M-CSF, IL-6, and IL-7 in vitro. A recent report stated that human B-cell progenitors obtained from cultures of cord blood $CD34^+CD10^-CD19^-$ cells gave rise to macrophages, NK cells, and T cells when exposed to the appropriate culture conditions.[23] Our study shows the lineage switch of human primary postnatal cells and further extends the existence of lineage switch to postmitotic cells. This notion is also supported by our observations in the microarray analysis that gene expression profiles of the resultant cells differed from those of the starting $CD15^+CD14^-$ neutrophils and were similar to those of $CD14^+$ cell–derived macrophages.

When we first cultured $CD15^+CD14^-$ neutrophils in the presence of GM-CSF, TNF-α, IFN-γ, and M-CSF, the resultant cells displayed morphologic and cytochemical features of macrophages. However, they preserved a low level of MPO activity and lactoferrin expression, as determined by flow cytometry. These data suggest that the resultant cells did not fully exhibit the phenotypic characteristics of macrophages. Our surprise was that the addition of IL-4 to cultures was sufficient for the resultant cells to acquire typical features of macrophages. It is also of note that in the presence of IL-4, the yield of the resultant cells increased to approximately 15%. The phagocytic activity of macrophages generated in IL-4–containing cultures was of a similar magnitude compared with that observed with $CD14^+$ cell–derived macrophages. Previous studies demonstrated the inhibitory activities of IL-4 on the development of monocytes/macrophages from progenitors supported by GM-CSF.[39,40] IL-4 has the potential to suppress TNF-α–induced effects on hematopoietic cells.[41] IL-4 also down-regulates the expression of 2 distinct receptors for TNF-α, p60, and p80 and induces shedding of these receptors, resulting in blockage of the cellular signaling elicited by TNF-α.[42] Moreover, several investigators have shown that IL-4 antagonizes IFN-γ–induced responses in human myeloid progenitor and mature cells.[43-45] Therefore, we have no plausible explanation for the mechanism of action of IL-4 on $CD15^+CD14^-$ neutrophils during their lineage switch to macrophages. Complex networks by multiple cytokines may be involved in the generation of macrophages from $CD15^+CD14^-$ neutrophils. Interestingly, phenotypic analysis indicated that when $CD15^+CD14^-$ neutrophils turn their lineage toward macrophages, they lose CD15 expression and acquire CD14. This finding demonstrates that the down-regulation of CD15 occurs before the up-regulation of CD14. The cascade of several different events may lead to the lineage conversion of $CD15^+CD14^-$ neutrophils to macrophages.

Our concern was whether a rare population of hematopoietic progenitors, contaminating the $CD15^+CD14^-$ fraction, could proliferate and differentiate into macrophages. If such were the case, the cultured cells would show signs of proliferation at several time points during culture. To address this issue, we used Ki-67 antibody staining, BrdU incorporation, and CFSE labeling. Neither $Ki-67^+$ nor $BrdU^+$ cells were detectable throughout culture, suggesting that cell division did not occur. In addition, if cultured cells had a history of successive cell divisions, we would have expected to observe separate peaks of CFSE fluorescence in the histogram. However, the narrow peak was observed with the resultant cells, as was the peak seen with the starting cell population. On the basis of these data and because the yield was approximately 15%, we assumed it was not possible for the cultured cells to have undergone more than one division throughout culture. Therefore, we propose that the generation of macrophages from $CD15^+CD14^-$ neutrophils with GM-CSF, TNF-α, IFN-γ, IL-4, and M-CSF was not caused by contamination of progenitor cells for macrophages but was the result of their lineage switch to macrophages. It was also possible that a small number of monocyte/macrophage precursors contaminated the starting $CD15^+CD14^-$ cell population. The yield in culture of $CD15^+CD14^-$ cells with M-CSF and neutrophilic features of a marginal number of the surviving cells could conceivably exclude this possibility.

Our observation that postmitotic neutrophils could generate macrophages raises the issue of developmental origin of human macrophages and may represent another developmental pathway from hematopoietic stem cells toward macrophages. However, it is unclear whether such a neutrophil-to-macrophage lineage switch occurs under physiologic conditions. Such a lineage switch may occur under specified conditions, such as inflammation, because GM-CSF, TNF-α, IFN-γ, IL-4, and M-CSF are inflammatory cytokines. Oehler et al[46] demonstrate that neutrophil granulocyte-committed cells acquire dendritic cell features in the presence of GM-CSF, IL-4, and TNF-α. Our results indicated that when $CD15^+CD14^-$ cells were cultured with GM-CSF, TNF-α, IFN-γ, and IL-4, the resultant cells exhibited a partial appearance of macrophages. IFN-γ may play a crucial role in the conversion of neutrophils into the macrophage lineage. In addition, it seems that neutrophils are capable of generating more types of mature cells than is generally recognized. Further studies on the reprogramming of already differentiated cells into other cell types are expected to yield new insights into events related to human hematopoiesis.

References

1. Metcalf D. The molecular control of cell division, differentiation commitment and maturation in haemopoietic cells. Nature. 1989;339:27-30.

2. Ogawa M. Differentiation and proliferation of hematopoietic stem cells. Blood. 1993;81:2844-2853.

3. Boyd AW, Schrader JW. Derivation of macrophagelike lines from the pre-B lymphoma ABLS 8.1 using 5-azacytidine. Nature. 1982;297:691-693.

4. Klinken SP, Alexander WS, Adams JM. Hemopoietic lineage switch: v-raf oncogene converts Eμ-myc transgenic B cells into macrophages. Cell. 1988;53:857-867.

5. Borzillo GV, Ashmun RA, Sherr CJ. Macrophage lineage switching of murine early pre-B lymphoid cells expressing transduced fms genes. Mol Cell Biol. 1990;10:2703-2714.

6. Lindeman G., Adams JM, Cory S, Harris AW. B-lymphoid to granulocytic switch during hematopoiesis in a transgenic mouse strain. Immunity. 1994;1:517-527.

7. Nutt SL, Heavey B, Rolink AG, Busslinger M. Commitment to the B-lymphoid lineage depends on the transcription factor Pax5. Nature. 1999; 401:556-562.

8. Rolink AG, Nutt SL, Melchers F, Busslinger M. Long-term in vivo reconstitution of T-cell development by Pax5-deficient B-cell progenitors. Nature. 1999;401:603-606.

9. Kee BL, Murre C. Induction of early B cell factor (EBF) and multiple B lineage genes by the basic helix-loop-helix transcriptional factor E12. J Exp Med. 1998;188:699-713.

10. Kondo M, Scherer DC, Miyamoto T, et al. Cell-fate conversion of lymphoid-committed progenitors by instructive actions of cytokines. Nature. 2000;407:383-386.

11. Iwasaki-Arai J, Iwasaki M, Miyamoto T, Watanabe S, Akashi K. Enforced granulocyte/macrophage colony-stimulating factor signals do not support lymphopoiesis, but instruct lymphoid to myelomonocytic lineage conversion. J Exp Med. 2003;197:1311-1322.

12. Iwasaki J, Mizuno S-I, Wells RA, Cantor AB, Watanabe S, Akashi K. GATA-1 converts lymphoid and myelomonocytic progenitors into the megakaryocyte/erythrocyte lineages. Immunity. 2003;19:451-462.

13. Visvader JE, Elefanty AG, Strasser A, Adams JM. GATA-1 but not SCL induces megakaryocytic differentiation in an early myeloid line. EMBO J. 1992;11:4557-4564.

14. Kulessa H, Frampton J, Graf T. GATA-1 reprograms avian myelomonocytic cell lines into eosinophils, thromboblasts, and erythroblasts. Genes Dev. 1995;9:1250-1262.

15. Seshasayee D, Gaines P, Wojchowski DM. GATA-1 dominantly activates a program of erythroid gene expression in factor-dependent myeloid FDCW2 cells. Mol Cell Biol. 1998;18:3278-3288.

16. Yamaguchi Y, Zon LI, Ackerman SJ, Yamamoto M, Suda T. Forced GATA-1 expression in the murine myeloid cell line M1: induction of c-Mpl expression and megakaryocytic/erythroid differentiation. Blood. 1998;91:450-457.

17. Yamada T, Kihara-Negishi F, Yamamoto H, Yamamoto M, Hashimoto Y, Oikawa T. Reduction of DNA binding activity of the GATA-1 transcriptional factor in the apoptotic process induced by overexpression of PU.1 in murine erythroleukemia cells. Exp Cell Res. 1998;245:186-194.

18. Muller C, Kowenz-Leutz E, Grieser-Ade S, Graf T, Leutz A. NF-M (chicken C/EBPβ) induces eosinophilic differentiation and apoptosis in a hematopoietic progenitor cell line. EMBO J. 1995;14:6127-6135.

19. Nerlov C, McNagny KM, Döderlein G, Kowenz-Leutz E, Graf T. Distinct C/EBP functions are required for eosinophilic lineage commitment and maturation. Genes Dev. 1998;12:2413-2423.

20. Querfurth E, Schuster M, Kulessa H, et al. Antagonism between C/EBPβ and FOG in eosinophil lineage commitment of multipotent hematopoietic progenitors. Genes Dev. 2000;14:2515-2525.

21. Montecino-Rodriguez E, Leathers H, Dorshkind K. Bipotential B-macrophages progenitors are present in adult bone marrow. Nat Immunol. 2001;2:83-88.

22. Lee C-K, Kim JK, Kim Y, et al. Generation of macrophages from early T progenitors in vitro. J Immunol. 2001;166:5964-5969.

23. Reynaud D, Lefort N, Manie E, Coulombel L, Levy Y. In vitro identification of human pro-B cells that give rise to macrophages, natural killer cells, and T cells. Blood. 2003;101:4313-4321.

24. Mahmud N, Katayama N, Nishii K, et al. Possible involvement of bcl-2 in regulation of cell-cycle progression of haemopoietic cells by transforming growth factor-β1. Br J Haematol. 1999;105:470-477.

25. Kovacs B, Maus MV, Riley JL, et al. Human CD8+ T cells do not require the polarization of lipid rafts for activation and proliferation. Proc Natl Acad Sci U S A. 2002;99:15006-15011.

26. Ohmine K, Ota J, Ueda M, et al. Characterization of stage progression in chronic myeloid leukemia by DNA microarray with purified hematopoietic stem cells. Oncogene. 2001;20:8249-8257.

27. Makishima H, Ishida F, Ito T, et al. DNA microarray analysis of T cell-type lymphoproliferative disease of granular lymphocytes. Br J Haematol. 2002;118:462-469.

28. Araki H, Katayama N, Mitani H, et al. Efficient ex vivo generation of dendritic cells from CD14+ blood monocytes in the presence of human serum albumin for use in clinical vaccine trials. Br J Haematol. 2001;114:681-689.

29. Oda T, Maeda H. A new simple fluorometric assay for phagocytosis. J Immunol Methods. 1986;88:175-183.

30. Metcalf D. Control of granulocytes and macrophages: molecular, cellular, and clinical aspects. Science. 1991;254:529-533.

31. Motoyoshi K. Biological activities and clinical application of M-CSF. Int J Hematol. 1997;67:109-122.

32. Witsell AL, Schook LB. Tumor necrosis factor α is an autocrine growth regulator during macrophage differentiation. Proc Natl Acad Sci U S A. 1992;89:4754-4758.

33. Tracey KJ, Cerami A. Tumor necrosis factor: a pleiotropic cytokine and therapeutic target. Annu Rev Med. 1994;45:491-503.

34. Friedman RM, Vogel SN. Interferons with special emphasis on the immune system. Adv Immunol. 1983;34:97-140.

35. Trinchieri G, Perussia B. Immune interferon: a pleiotropic lymphokine with multiple effects. Immunol Today. 1985;6:131-136.

36. Schreiber RD, Celada A. Molecular characterization of interferon γ as a macrophage activating factor. Lymphokines. 1985;11:87-118.

37. Alon U, Barkai N, Notterman DA, et al. Broad pat-

terns of gene expression revealed by clustering analysis of tumor and normal colon tissues probed by oligonucleotides arrays. Proc Natl Acad Sci U S A. 1999;96:6745-6750.

38. Brons PPT, Raemaekers JMM, Bogman JJT, et al. Cell cycle kinetics in malignant lymphoma studied with in vivo iododeoxyuridine administration, nuclear Ki-67 staining, and flow cytometry. Blood. 1992;80:2336-2343.

39. Jansen JH, Wientjens G-JHM, Fibbe WE, Willemze R, Kluin-Nelemans HC. Inhibition of human macrophage colony formation by interleukin 4. J Exp Med. 1989;170:577-582.

40. Snoeck H-W, Lardon F, Van Bockstaele DR, Peetermans ME. Effects of interleukin-4 (IL4) on myelopoiesis: studies on highly purified CD34+ hematopoietic progenitor cells. Leukemia. 1993;7:625-629.

41. Levesque MC, Haynes BF. Cytokine induction of the ability of human monocyte CD44 to bind hyaluronan is mediated primarily by TNF-α and inhibited by IL-4 and IL-13. J Immunol. 1997;159:6184-6194.

42. Manna SK, Aggarwal BB. Interleukin-4 downregulates both forms of tumor necrosis factor receptor and receptor-mediated apoptosis, NF-κB, AP-1, and c-Jun N-terminal kinase. J Biol Chem. 1998;273:33333-33341.

43. te Velde AA, Huijbens RJF, de Vries JE, Figdor CG. IL-4 decreases FcγR membrane expression and FcγR-mediated cytotoxic activity of human monocytes. J Immunol. 1990;144:3046-3051.

44. te Velde AA, Huijbens RJF, Heije K, de Vries JE, Figdor CG. Interleukin-4 (IL-4) inhibits secretion of IL-1β, tumor necrosis factor α, and IL-6 by human monocytes. Blood. 1990;76:1392-1397.

45. Snoeck H-W, Lardon F, Lenjou M, Nys G, Van Bockstaele DR, Peetermans ME. Interferon-γ and interleukin-4 reciprocally regulate the production of monocytes/macrophages and neutrophils through a direct effect on committed monopotential bone marrow progenitor cells. Eur J Immunol. 1993;23:1072-1077.

46. Oehler L, Majdic O, Pickl WF, et al. Neutrophil granulocyte-committed cells can be driven to acquire dendritic cell characteristics. J Exp Med. 1998;187:1019-1028.

Mutual Regulation of Protein-tyrosine Phosphatase 20 and Protein-tyrosine Kinase Tec Activities by Tyrosine Phosphorylation and Dephosphorylation*

Naohito Aoki‡§, Shuichi Ueno¶, Hiroyuki Mano¶, Sho Yamasaki‖, Masayuki Shiota**,
Hitoshi Miyazaki**, Yumiko Yamaguchi-Aoki‡‡, Tsukasa Matsuda‡, and Axel Ullrich‡‡

From the ‡Department of Applied Molecular Biosciences, Graduate School of Bioagricultural Sciences, Nagoya University,
Furo-cho, Chikusa-ku, Nagoya 464-8601, Japan, ¶Divisions of Functional Genomics, Cardiology and Hematology,
Jichi Medical School, Kawachi-gun, Tochigi 329-0498, Japan, ‖Molecular Genetics, Chiba University Graduate
School of Medicine, Chiba 260-8670, Japan, **Gene Research Center, University of Tsukuba, Ibaraki 305-8572, Japan,
and ‡‡Max Planck Institute for Biochemistry, Department of Molecular Biology, D-82152 Martinsried, Germany

PTP20, also known as HSCF/protein-tyrosine phosphatase K1/fetal liver phosphatase 1/brain-derived phosphatase 1, is a cytosolic protein-tyrosine phosphatase with currently unknown biological relevance. We have identified that the nonreceptor protein-tyrosine kinase Tec-phosphorylated PTP20 on tyrosines and co-immunoprecipitated with the phosphatase in a phosphotyrosine-dependent manner. The interaction between the two proteins involved the Tec SH2 domain and the C-terminal tyrosine residues Tyr-281, Tyr-303, Tyr-354, and Tyr-381 of PTP20, which were also necessary for tyrosine phosphorylation/dephosphorylation. Association between endogenous PTP20 and Tec was also tyrosine phosphorylation-dependent in the immature B cell line Ramos. Finally, the Tyr-281 residue of PTP20 was shown to be critical for deactivating Tec in Ramos cells upon B cell receptor ligation as well as dephosphorylation and deactivation of Tec and PTP20 itself in transfected COS7 cells. Taken together, PTP20 appears to play a negative role in Tec-mediated signaling, and Tec-PTP20 interaction might represent a negative feedback mechanism.

Protein-tyrosine phosphatases (PTPs)[1] are a large and structurally diverse family of enzymes that catalyze the dephosphorylation of tyrosine-phosphorylated proteins (1, 2). Biochemical and kinetic studies have documented that Cys and an Asp residues in the catalytic domain are essential for the PTP activity. PTPs have been shown to participate as either positive or negative regulators of signaling pathways in a wide range of physiological processes, including cellular growth, differentia-

tion, migration, and survival (1, 2). Despite their important roles in such fundamental cellular processes, the mechanisms by which PTPs exert their effects are largely not understood.

PTP20 (3), which is also known as hematopoietic stem cell fraction (HSCF) (4), PTP-K1 (5), fetal liver phosphatase 1 (6), and brain-derived phosphatase 1 (7), comprises the PEST family of PTPs together with PTP-PEST and PEP PTP and was originally isolated by screening a PC12 cDNA library. Overexpression of PTP20 in PC12 cells results in a more rapid and robust neurite outgrowth in response to nerve growth factor treatment, suggesting that PTP20 is involved in cytoskeletal reorganization (3). Mostly consistent with this observation, overexpression of a dominant negative mutant of fetal liver phosphatase 1 in K562 hematopoietic progenitor cells results in an inhibition of cell spreading and substrate adhesion in response to phorbol ester (6). Recently, through yeast two-hybrid screening the proline, serine, threonine phosphatase-interacting protein (PSTPIP) and PSTPIP2 have been identified to be specific in vivo substrates for HSCF, because the phosphotyrosine (Tyr(P)) level of PSTPIP1 is significantly enhanced by coexpression of the catalytically inactive mutant (Cys to Ser) of PTP20 (8, 9). PSTPIP is tyrosine-phosphorylated both in BaF3 cells and in v-Src-transfected COS cells and is shown to be co-localized with the cortical actin cytoskeleton, lamellipodia, and actin-rich cytokinetic cleavage furrow (8), strongly supporting the idea that PTP20/HSCF is a potential regulator of cytokinesis. PSTPIP also interacts with the C-terminal part of the cytosolic protein-tyrosine kinase (PTK) c-Abl, serves as a substrate for c-Abl, and can bridge interactions between c-Abl and PTP20 with the dephosphorylation of c-Abl by PTP20 (10). It has also been reported that PTP20 associates with the negative Src-family kinase regulator Csk via its Src homology 2 (SH2) domain and two putative sites of tyrosine phosphorylation of the phosphatase (11). This association is thought to allow Csk and PTP20 to synergistically inhibit Src-family kinase activity by phosphorylating and dephosphorylating negative and positive regulatory tyrosine residues, respectively.

Regarding post-translational regulation of the PEST family PTPs, it has been documented that phosphorylation of an N-terminal serine residue, which is well conserved in all members of the PEST PTP family, by protein kinase A results in the inhibition of its catalytic activity (12). In addition to proline, serine, and threonine residues in the C-terminal PEST domain of PTP20, a large number of tyrosine residues exist in that region, suggesting the possibility that PTP20 is tyrosine-phosphorylated. Indeed, previous studies reveal that PTP20/HSCF

[1] The abbreviations used are: PTP, protein-tyrosine phosphatase; HSCF, hematopoietic stem cell fraction; PSTPIP, proline, serine, threonine phosphatase-interacting protein; PTK, protein-tyrosine kinase; BCR, B cell receptor; SH2, Src homology 2; SH3, Src homology 3; HA, hemagglutinin; GST, glutathione S-transferase; WT, wild type; ECL, enhanced chemiluminescence; PH, pleckstrin homology; TH, Tec homology; POV, pervanadate.

becomes tyrosine-phosphorylated by constitutively active forms of Lck and v-Src kinases in transfected cells (8, 11) even though the physiological relevance of tyrosine phosphorylation on PTP20 remains unclear.

In this study we addressed the question of PTP20 regulation with special emphasis on the relevance of tyrosine phosphorylation and its biological impact. Through co-expression with nonreceptor PTKs we found that Tec kinase strongly tyrosine-phosphorylated the catalytically inactive form of PTP20 and that Tec physically interacted with PTP20 in a tyrosine phosphorylation-dependent manner in transfected COS7 cells. Further analyses with a variety of mutants of PTP20 and Tec revealed that C-terminal tyrosine residues of PTP20 and the Tec SH2 domain were necessary in the regulation of respective state of phosphorylation. Ectopic expression of PTP20 in human immature Ramos B cells resulted in suppression of B-cell receptor-induced c-*fos* promoter activity. Moreover, we determined that tyrosine 281 of PTP20 played a role in the dephosphorylation activity of PTP20 against both Tec and PTP20 itself. Our findings suggest a negative feedback mechanism that mutually controls the tyrosine phosphorylation of Tec and PTP20 and regulates Tec activity and B cell receptor (BCR) signaling.

EXPERIMENTAL PROCEDURES

Reagents—Antibodies to hemagglutinin (HA) epitope (Y-11), phosphotyrosine (PY99), glutathione S-transferase (GST) (Z-5), Src (SRC2), Lck (2102), JAK2 (M-126), JAK3 (C-21), Csk (C-20), and ZAP70 (LR) were purchased from Santa Cruz Biotechnology Inc. (Santa Cruz, CA). Antibodies to Tec, Itk, Btk, and Bmx were as described previously (13). Antibody to PTP20 was prepared by immunizing rabbits with the N-terminal peptide of PTP20 (MSRQSDLVRSFLEQQEARDH), to which a cysteine residue was added to the C terminus, coupled to keyhole limpet hemocyanin (14). Anti-human IgM antibody (Fab')$_2$ fragment was obtained from Southern Biotechnology Associates (Birmingham, AL). All other reagents were from Sigma unless otherwise noted.

Plasmid Construction—The pSR-based expression vectors for Tec wild-type (WT), Tec kinase mutant, TecY187F, TecY518F, and Tec proteins lacking each subdomain were described previously (15, 16). pEBG plasmids (17) encoding each subdomain of Tec to express the GST-tagged proteins were previously described (18). HA epitope tagging to PTP20 at its N terminus and subsequently all the mutations (cysteine to serine, aspartic acid to alanine, and tyrosine to phenylalanine) in PTP20 were carried out by PCR-based strategy. To express GST-tagged PTP20 in mammalian cells, full-length PTP20 (amino acids 2–453), PTP catalytic domain (amino acids 2–308), and the C-terminal noncatalytic PEST domain (amino acids 271–453) were amplified by PCR and ligated into pEBG vector via the BamHI site. All the plasmids newly constructed were confirmed by sequencing. Expression plasmids for rat Csk and mouse JAK2 were generous gifts from Drs. M. Okada (Osaka University, Japan) and J. N. Ihle (St. Jude Children's Research Hospital, Memphis, TN), respectively. Expression plasmids for mouse Src, Lck, Itk, Btk, Bmx, ZAP-70, and JAK3 were described elsewhere.

Cell Culture and Transfection—COS7 cells were cultured in Dulbecco's modified Eagle's medium (high glucose, Sigma) supplemented with 10% fetal calf serum. Ramos cells (American Type Culture Collection, Manassas, VA) were maintained in RPMI 1640 medium (Invitrogen) supplemented with 10% fetal calf serum. Upon transfection experiments COS7 cells were inoculated at a density of 4×10^5 cells/6-cm dish and grown overnight in Dulbecco's modified Eagle's medium containing 10% fetal calf serum. Expression plasmids were transfected into the cells by the modified calcium phosphate precipitation method (19). After incubation under 3% CO_2, 97% air for 18 h, the transfected cells were washed with phosphate-buffered saline twice and cultured in fresh Dulbecco's modified Eagle's medium containing 10% fetal calf serum for another 24 h under humidified 5% CO_2 and 95% air.

Cell Lysis, Immunoprecipitation, GST Pull-down, and Western Blotting—The transfected cells were lysed with lysis buffer containing 50 mM Tris-HCl (pH 7.5), 5 mM EDTA, 150 mM NaCl, 10 mM sodium phosphate, 10 mM sodium fluoride, 1% Triton X-100, 1 mM phenylmethylsulfonyl fluoride, and 10 μg/ml leupeptin. Lysates were directly subjected to immunoblotting, immunoprecipitation with the indicated antibodies plus protein G- or Protein A-Sepharose beads (Amersham Bioscience), or precipitation with GSH-Sepharose beads (Amersham

Bioscience). Proteins in the immunoprecipitates and precipitates were further analyzed by immunoblotting with the indicated antibodies. The protein bands were visualized with an enhanced chemiluminescence (ECL) detection kit (Amersham Bioscience) and light capture system (AE-6962, ATTO, Tokyo, Japan).

c-fos Promoter Assay—Ramos cells (1×10^7/experiment) were subjected to electroporation with 2 μg of the pfos/luc reporter plasmid (20) plus 10 μg of expression plasmids for PTP20 or its mutants. Five hours after transfection cells were incubated for 5 h in the absence or presence of antibodies to human IgM (10 μg/ml). Luciferase activity was measured with the use of the dual luciferase assay system (Promega, Madison, WI).

RESULTS

Tec Is a Potent Regulator of PTP20—Although PTP20 has been shown to be a substrate of v-Src (8) and constitutively active Lck (11), the physiological relevance of PTP20 tyrosine phosphorylation remains unknown. Northern blot analysis revealed that PTP20 was abundantly expressed in spleen, suggesting a role in the immune system (data not shown). Therefore, it was reasoned that other PTKs of immune cells might be involved in PTP20 regulation by tyrosine phosphorylation. To examine this possibility HA-tagged PTP20 was co-expressed with various cytosolic PTKs including Src and Lck in COS7 cells. We used a catalytically inactive form of PTP20 for this experiment because autodephosphorylation activity of PTP20 has been previously reported (8). Cells were lysed, PTP20 was immunoprecipitated with anti-HA antibody, and the immune complexes were subjected to SDS-PAGE and immunoblotting with anti-phosphotyrosine antibody. As shown in Fig. 1A, PTP20 was tyrosine-phosphorylated by Src and Lck and co-immunoprecipitated with proteins with 56 and 60 kDa, likely corresponding to Lck and Src, respectively. In the case of ectopic Lck expression, endogenous Src seemed to be included in the immune complex, as suggested by the presence of a 66-kDa phosphotyrosine-containing band. PTP20 was slightly tyrosine-phosphorylated by Csk and co-immunoprecipitated with a faintly tyrosine-phosphorylated 70-kDa band, which seemed unlikely to be Csk. JAK2 but not JAK3 also tyrosine-phosphorylated PTP20 and appeared to be co-immunoprecipitated with PTP20. Most notably, PTP20 was strongly tyrosine-phosphorylated by Tec and co-immunoprecipitated with a heavily tyrosine-phosphorylated protein of 74 kDa and other minor proteins of 120 and 35 kDa. Based on the molecular mass, the 74-kDa protein was likely to represent Tec. Itk, another member of Tec/Btk family, also tyrosine-phosphorylated PTP20 to a lesser extent and was co-immunoprecipitated, whereas related PTKs Btk and Bmx did not tyrosine phosphorylate PTP20 and were not co-immunoprecipitated. Because all the transfected PTKs were obviously expressed as compared with mock transfectant (Fig. 1, *panel B*), it was suggested that Tec tyrosine-phosphorylated PTP20 with the greatest efficiency.

Tec Is a Potential Substrate of PTP20—To examine the relationship between PTP20 and Tec in more detail, Tec was co-transfected with WT or a catalytically inactive C/S form of PTP20 into COS7 cells, and either PTP20 or Tec was immunoprecipitated followed by immunoblotting with anti-phosphotyrosine antibody. When HA-PTP20 WT was expressed, no phosphorylated bands were visible in both anti-HA and anti-Tec immunoprecipitates, possibly due to dephosphorylation activity of PTP20 against both Tec and itself (Fig. 2). Two major bands with 74 and 50 kDa in the anti-HA and anti-Tec immune complexes were detected with anti-phosphotyrosine antibody only when the PTP20 C/S mutant was co-transfected with Tec. Reprobing with anti-Tec and anti-HA antibodies clearly revealed that the bands represent Tec and HA-PTP20. No phosphorylation of Tec was observed when Tec alone was introduced into COS7 cells, suggesting that the interaction between Tec and PTP20 was required for Tec phosphorylation and pos-
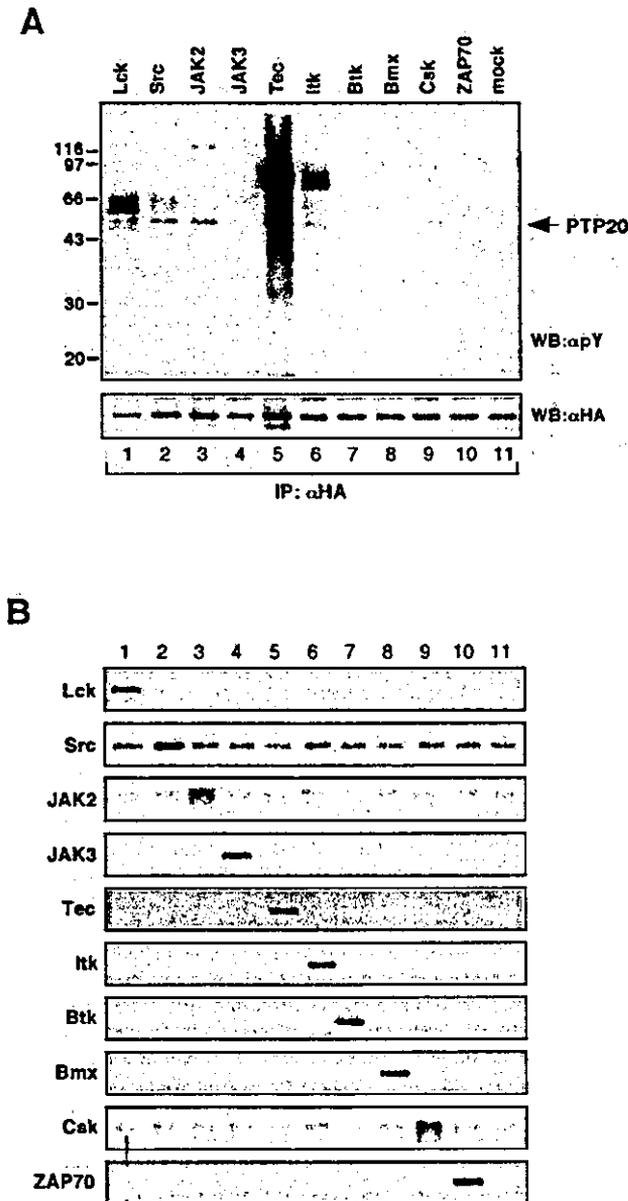
A

B

FIG. 1. Tyrosine phosphorylation of PTP20 by various PTKs. *A*, COS7 cells were transiently transfected with HA-PTP20 C/S together with either Lck, Src, JAK2, JAK3, Tec, Itk, Btk, Bmx, Csk, or ZAP70. Cells were lysed, and PTP20 was immunoprecipitated (*IP*) with anti-HA antibody followed by immunoblotting (*WB*) with anti-phosphotyrosine antibody (PY99 (*αpY*)). The same membrane was reprobed with anti-HA antibody after stripping. *B*, an aliquot of the cell lysates was immunoblotted with the indicated antibodies to confirm substantial expression of each PTK.

sibly activation. These results suggest that PTP20 is a substrate of Tec and that Tec is also a substrate of PTP20.

Phosphotyrosine-dependent Interaction between PTP20 and Tec—Tec is composed of several distinct domains including pleckstrin homology (*PH*), Tec homology (*TH*), SH3, SH2, and kinase (*KD*) domains (Fig. 3, *panel A*). All of these domains are necessary for full function of Tec under physiological conditions (15, 16). To examine which domains are involved in interaction with PTP20, Tec mutants each lacking one of the domains were co-transfected with the catalytically inactive form of PTP20 into COS7 cells. A kinase mutant as well as two mutants (Y187F and Y518F) where tyrosine residues were replaced by

phenylalanines were also included. Cells were lysed, and PTP20 was immunoprecipitated followed by immunoblotting with anti-phosphotyrosine antibody. PTP20 was tyrosine-phosphorylated by the Y187F mutant as well as mutants lacking PH, TH, and SH3 domains to a similar extent as compared with Tec WT (Fig. 3, *panel B*). As expected, the Y518F mutant, which is missing the autophosphorylation site for Tec activation, and the inactive mutant of a kinase mutant could not tyrosine phosphorylate PTP20. Interestingly, the ΔPH mutant could tyrosine phosphorylate PTP20 but was not co-immunoprecipitated with PTP20. Most strikingly, the ΔSH2 mutant could not tyrosine phosphorylate PTP20 and was not co-immunoprecipitated with PTP20. When a membrane on which aliquots of total cell lysates were blotted was probed with anti-phosphotyrosine antibody, it was revealed that co-expression of the Tec ΔSH2 mutant and PTP20 resulted in no tyrosine phosphorylation on both molecules and that the Tec ΔPH mutant tyrosine-phosphorylated (Fig. 3, *panel C*). Tec SH2 domain-dependent interaction with PTP20 was further investigated by co-transfecting the PTP20 C/S mutant with plasmids encoding GST fusion proteins of Tec domains in the presence or absence of Tec into COS7 cells. Cell lysates were subjected to pull-down experiments with GSH-Sepharose beads. Precipitates were separated by SDS-PAGE followed by immunoblotting with the indicated antibodies. In the absence of full-length Tec co-expression, no substantial binding of PTP20 to any of the Tec domains was apparent (Fig. 3, *panel D*). In contrast, in the presence of full-length Tec, phosphorylated PTP20 bound to only the SH2 domain of Tec. Given that co-expression of Tec should result in marked tyrosine phosphorylation of PTP20 in COS7 cells, these data indicate that the PTP20-Tec interaction is mediated predominantly by the SH2 domain of Tec and phosphotyrosine residues of PTP20.

Next, we tried to identify the binding site(s) for Tec in PTP20. Because the interaction of Tec with PTP20 was mediated by the Tec SH2 domain, potential tyrosine residues of phosphorylation were first taken into consideration. There are 13 tyrosine residues (Tyr-62, Tyr-68, Tyr-86, Tyr-101, Tyr-144, Tyr-192, Tyr-244, Tyr-281, Tyr-285, Tyr-303, Tyr-354, Tyr-381, Tyr-419) in the PTP20 sequence, and all the residues are perfectly conserved among human and mouse orthologs (Fig. 4). We focused our attention on the tyrosine residues Tyr-281, Tyr-285, Tyr-303, Tyr-354, Tyr-381, and Tyr-419 located in the C-terminal PEST domain of PTP20, and 6 residues were individually mutated.

First, the mutants were tested for the extent of tyrosine phosphorylation by Tec in transfected COS7 cells. Total cell lysates were subjected to anti-phosphotyrosine blotting. Fig. 5, *panel A*, demonstrates that the PTP20 mutants (Y281F, Y303F, Y354F, Y381F) in which Tyr-281, Tyr-303, Tyr-354, and Tyr-381 were individually mutated exhibited dramatic reduction in tyrosine phosphorylation levels, whereas no apparent reduction for Y285F and Y419F was observed. Combinational mutation of Tyr-281, Tyr-303, Tyr-354, and Tyr-381 totally abolished tyrosine phosphorylation of PTP20. In keeping with these data, anti-phosphotyrosine blotting also demonstrated that tyrosine phosphorylation of Tec was concomitantly reduced. This observation was further extended by GST pull-down experiments using the Tec SH2 domain. COS7 cells were then transfected with PTP20 YF variants together with Tec and Tec-Tec SH2, as outlined in Fig. 3, *panel C*. Mutation of either Tyr-281, Tyr-303, Tyr-354, or Tyr-381 of PTP20 resulted in reduced binding capacity of PTP20 to the Tec SH2 domain, and again, such binding was completely abrogated by substituting all the tyrosine residues (Fig. 5, *panel B*). Together these data clearly indicate that four tyrosine residues in the C-ter-

FIG. 2. **Tyrosine phosphorylation-dependent interaction of PTP20 with Tec.** Tec cDNA was transiently introduced into COS7 cells together with either empty vector (mock), HA-PTP20 WT, or C/S and lysed. PTP20 or Tec was immunoprecipitated either with anti-HA (*left panels*) or anti-Tec (*right panels*) antibody, respectively. The immunoprecipitates (*IP*) were separated by SDS-PAGE followed by immunoblotting (*WB*) sequentially with the indicated antibodies. The bands corresponding to Tec and PTP20 are indicated by *arrows*. In either case expression of Tec or HA-PTP20 was confirmed using aliquots of total cell lysates (*TCL*) by immunoblotting (*lowest panels*). *apY*, anti-phosphotyrosine antibody.
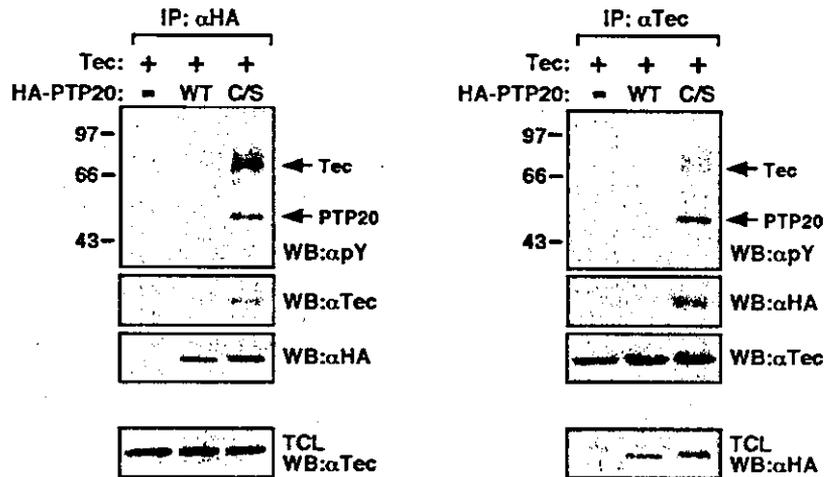
minal non-catalytic region of PTP20 are involved in not only binding to the Tec SH2 domain but also in the phosphorylation and subsequent activation of Tec.

We asked whether the C-terminal non-catalytic region of PTP20 was enough for phosphorylation and activation of Tec. To this end, PTP20 deletion mutants lacking either an N-terminal catalytic or a C-terminal non-catalytic segment were made, but the resultant constructs could not be expressed in COS7 cells, although comparable amounts of transcripts were detected (data not shown). To solve this problem, the N-terminal PTP domain and the C-terminal PEST domain were inserted into pEBG vector and were expressed as GST fusion proteins in COS7 cells. These pEBG plasmids encoding the PTP domain and full length of PTP20 C/S mutant and the PEST domain of PTP20 were co-transfected into COS7 together with Tec. Anti-phosphotyrosine blotting documented that Tec was highly tyrosine-phosphorylated with the full-length but not the PTP domain of the PTP20 C/S mutant (Fig. 6, *panel A*), supporting previous data shown in Fig. 5, where the C-terminal part of PTP20 was essential for tyrosine phosphorylation of Tec. Interestingly, the presence of the PEST domain of PTP20 caused tyrosine phosphorylation of PTP20, but the extent was lower than in the presence of the full-length PTP20 C/S mutant. Equivalent expression of each construct was confirmed by Western blotting with anti-Tec and anti-GST antibodies. To further examine the involvement of the PEST domain, lysates were precipitated with GSH-Sepharose beads followed by immunoblotting with anti-phosphotyrosine antibody. A phosphorylated 74-kDa band, which was shown to be Tec by immunoblotting, was co-precipitated with full-length PTP20 C/S mutant, whereas the PTP domain alone could not capture Tec (Fig. 6, *panel B*). A faint tyrosine-phosphorylated band with the same mobility of 74 kDa that co-precipitated with the PEST domain appeared to be Tec but could not be detected by our anti-Tec antibody presumably due to sensitivity. These results suggest that the PEST domain of PTP20 is necessary but not sufficient for not only hyperphosphorylation and activation of, but also association with Tec.

Negative Regulatory Roles of PTP20 in BCR Signaling—All the experiments documented above were conducted in transfected COS7 cells. To demonstrate a physiological relevance of the PTP20-Tec interaction, evidence of such an association in non-transfected cells was required. To this end we selected human Ramos immature B cells, because it has been reported that they express relatively high amounts of endogenous Tec (21). As shown above, interaction of PTP20 with Tec is mediated by tyrosine phosphorylation of PTP20, and PTP20 has autodephosphorylation activity, implying that it would be dif-

ficult to detect a phosphotyrosine-dependent interaction of PTP20 with other molecules including Tec endogenously. To overcome this experimental difficulty, protein-tyrosine phosphorylation was induced in Ramos cells by treatment with pervanadate (POV). Cells were starved for 16 h in serum-free medium and then either left unstimulated or treated with 0.1 mM POV for 30 min and lysed. Cell lysates were immunoprecipitated with either anti-phosphotyrosine antibody or anti-Tec antibody. Our PTP20-specific antibody could not be used due to its inability in immunoprecipitation experiments. In anti-phosphotyrosine immunoprecipitates, specific bands with 74 and 50 kDa corresponding to human Tec and PTP20 were detected only upon POV treatment (Fig. 7). A tyrosine-phosphorylated band with 50 kDa in the anti-Tec immunoprecipitates was readily detected by the anti-PTP20 antibody but only when cells received POV pretreatment (Fig. 7). These results indicate that endogenous Tec and PTP20 interact with each other in a phosphotyrosine-dependent manner in Ramos B cells.

Although upstream regulators such as cytokine receptors, lymphocyte surface antigens, G protein-coupled receptors, receptor type PTKs, or integrins for Tec in blood cells including Ramos B cells have been relatively well investigated (13, 20, 22–26), only limited information regarding downstream regulators of Tec has been available so far. If the data obtained in transfected COS7 cells are true, PTP20 would be thought to play a negative regulatory role in Tec-mediated signaling. To examine this, either the PTP20 WT, the inactive C/S mutant, or another form of catalytically inactive mutant D/A was transiently co-transfected with the pfos/luc reporter plasmid into Ramos cells, because the promoter of the c-*fos* proto-oncogene is activated in response to BCR cross-linking in the cells. Cells were either left unstimulated or treated with anti-human IgM F(ab')₂ fragments for 5 h. Cell lysates were assayed for luciferase activity. BCR cross-linking induced a marked activation of the c-*fos* promoter (Fig. 8). Expression of PTP20 WT totally inhibited BCR-induced activation of the c-*fos* promoter as well as its basal activity, whereas only about 20% inhibition of the promoter activation was observed in the co-expression of catalytically inactive forms of PTP20, strongly indicating that PTP20 is a negative regulator of BCR-Tec-c-*fos* signaling.

Tyrosine Phosphorylation of PTP20 by Tec Modulates Its Catalytic Activity against Tec as Well as Itself—We demonstrated that specific tyrosine residues Tyr-281, Tyr-303, Tyr-354, and Tyr-381 of PTP20 could be phosphorylated by Tec and served as Tec binding sites (Fig. 5). To further investigate physiological relevance of PTP20 tyrosine phosphorylation, substitution of the tyrosine residues with phenylalanine in PTP20 WT was performed. The YF mutants of HA-PTP20 WT
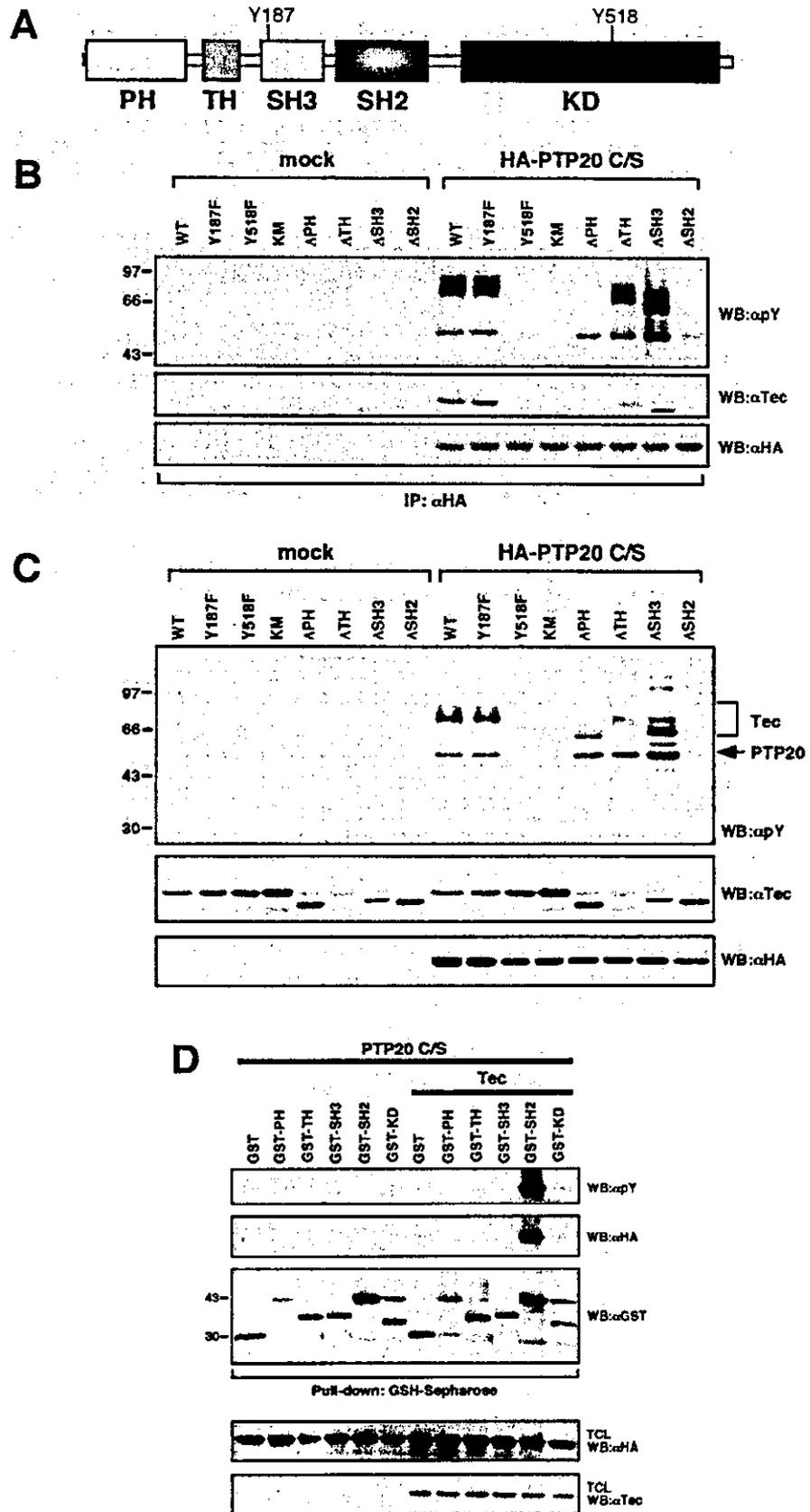
A

B

FIG. 3. Tec SH2 domain is essential for both tyrosine phosphorylation of PTP20 and association of Tec with PTP20. *A*, schematic organization of mouse Tec into PH, TH, SH3, SH2, and kinase (*KD*) domains. *B*, COS7 cells were transiently transfected with either empty vector (*mock*) or HA-PTP20 C/S together with the indicated Tec mutants. Cells were lysed, and HA-PTP20 was immunoprecipitated (*IP*) followed by immunoblotting (*IB*) with anti-phosphotyrosine antibody (PY99 (*αpY*)). The same membrane was sequentially reprobed with anti-Tec and anti-HA antibodies after stripping. *C*, aliquots of the total cell lysates (*TCL*) were separated by SDS-PAGE followed by immunoblotting with indicated antibodies. *D*, COS7 cells were transiently transfected with pEBG empty vector (GST) or bearing each of Tec domains (PH, TH, SH3, SH2, and KD) in the absence or presence of Tec plasmid. Cells were lysed, and GST fusion proteins were precipitated by GSH-Sepharose beads followed by immunoblot analysis with anti-phosphotyrosine (*pY*) antibody. The same membrane was sequentially reprobed with indicated antibodies. Expression of PTP20 and Tec was confirmed using aliquots of total cell lysates (*TCL*) by immunoblotting as indicated.

C

D

```
                 62     68                          86                    101
PTP20(rat)   MSRQSDLVRS FLEQQEARDH RKGAILAREF SDIKARSVAW KTEGVCSTKA GSQQGNSKKN  60
HSCF(mouse)  MSRHTDLVRS FLEQLEARDY REGAILAREF SDIKARSVAW KSEGVCSTKA GSRLGNTNKN  60
BDP1(human)  MSRSLDSARS FLERLEARGG REGAVLAGEF SDIQACSAAW KADGVCSTVA GSRPENVRKN  60

PTP20(rat)   RYKDVVPYDE TRVILSLLQE EGHGDMINAN FIRGTDGSQA MIATQGPLPH TLLDFWRLVW 120
HSCF(mouse)  RYKDVVAYDE TRVILSLLQE EGHGDMINAN FIRGIDGSQA MIATQGPLPH TLLDFWRLVW 120
BDP1(human)  RYKDVLPYDQ TRVILSLLQE EGHSDMINGN FIRGVDGSLA MIATQGPLPH TLLDFWRLVW 120

                                            144
PTP20(rat)   EFGIKVILMA CQETENGRRK CERMWAQERE PLQAGPFCIT LTKETALTSD ITLRTLQVTF 180
HSCF(mouse)  EFGVKVILMA CQETENGRRK CERMWAREQE PLKAGPFCIT LTKETTLNAD ITLRTLQVTF 180
BDP1(human)  EFGVKVILMA CREIENGRKR CERMWAQEQE PLQTGLFCIT LIKEKWLNED IMLRTLKVTF 180

                              192
PTP20(rat)   QKESRPVHQL QYMSWPDHGV PSSSDHILTM VEEARCLQGL GPGPLCVHCS AGCGRTGVLC 240
HSCF(mouse)  QKEFRSVHQL QYMSWPDHGV PSSSDHILTM VEEARCLQGL GPGPLCVHCS AGCGRTGVLC 240
BDP1(human)  QKESRSVYQL QYMSWPDRGV PSSPDHMLAM VEEARRLQGS GPEPLCVHCS AGCGRTGVLC 240

                244                                          281 285
PTP20(rat)   AVDYVRQLLL TQTIPPNFSL FEVVLEMRKQ RPAAVQTEEQ YRFLYHTVAQ LFSRTLQNNS 300
HSCF(mouse)  AVDYVRQLLL TQTIPPNFSL FQVVLEMRKQ RPAAVQTEEQ YRFLYHTVAQ LFSRTLQDTS 300
BDP1(human)  TVDYVRQLLL TQMIPPDFSL FDVVLKMRKQ RPAAVQTEEQ YRFLYHTVAQ MPCSTLQNAS 300

             303                                                        354
PTP20(rat)   PLYQNLKENR APICKDSSSL RTSSALPATS RPLGGVLRSI SVPGPPTLPM ADTYAVVQKR 360
HSCF(mouse)  PHYQNLKENC APICKEAFSL RTSSALPATS RPPGGVLRSI SVPAPPTLPM ADTYAVVQKR 360
BDP1(human)  PHYQNIKENC APLYDDALFL RTPQALLAIP RPPGGVLRSI SVPGSPGHAM ADTYAVVQKR 360

                                            381
PTP20(rat)   GASGSTGPGT RAPNST---- --DTPIYSQV APRIQRPVSH TENAQGTTAL GRVPADENPS 414
HSCF(mouse)  GASAGTGPGP RAPTST---- --DTPIYSQV APRAQRPVAH TEDAQGTTAL RRVPADQNSS 414
BDP1(human)  GAPAGAGSGT QTGTGTGARS AEEAPLYSKV TPRAQRPGAH AEDARGTLP- GRVPADQSPA 420

             419
PTP20(rat)   GPDAYEEVTD GAQTGGLGFN LRIGRPKGPR DPPAEWTRV 453
HSCF(mouse)  GPDAYEEVTD GAQTGGLGFN LRIGRPKGPR DPPAEWTRV 453
BDP1(human)  GSGAYEDVAG GAQTGGLGFN LRIGRPKGPR DPPAEWTRV 458
```

FIG. 4. **Sequence alignment of PTP20 with its human (brain-derived phosphatase 1 (*BDP1*)) and mouse (*HSCF*) orthologs.** The 13 conserved tyrosine residues are *boxed* and *numbered* based on the amino acid sequence of PTP20. PTP catalytic domains are indicated by *gray shading*.

were co-transfected with Tec and the PTP20 C/S mutant without epitope tagging, and effects on the extent of tyrosine phosphorylation on Tec were analyzed by anti-phosphotyrosine blotting. As shown in Fig. 9A, substitution of Tyr-281 with phenylalanine (Y281F) resulted in dramatic loss of PTP20 dephosphorylation activity against Tec. On the other hand, Tec could be dephosphorylated by Y303F, Y354F, and Y381F to nearly the same extent by PTP20 WT. The PTP20 Y281F/Y303F/Y354/F381F mutant in which 4 tyrosine residues were substituted by phenylalanine also exhibited apparently no dephosphorylation activity against Tec. Equivalent expression of HA-PTP20 was confirmed by immunoblotting (*lowest panel*). Next, the autodephosphorylation activity of the YF mutants of HA-PTP20 WT was assessed by co-transfecting Tec and-PEST encoding the GST-PTP20 PEST domain into COS7 cells, as GST-PTP20 PEST alone became tyrosine-phosphorylated in the presence of Tec (Fig. 6). Cells were lysed and GST-PTP20 PEST was precipitated with GSH-Sepharose beads followed by anti-phosphotyrosine blotting. Again, PTP20 Y281F as well as PTP20 Y281F/Y303F/Y354/F381F showed no dephosphorylation activity against GST-PTP20 PEST, whereas PTP20 Y303F, Y354F, and Y381F as well as PTP20 WT could dephosphorylate GST-PTP20 PEST (Fig. 9B). These YF mutants also were transfected into Ramos B cells, and c-*fos* promoter activity was assayed after BCR ligation. Ectopic expression of PTP20 Y281F and Y281F/Y303F/Y354/F381F mutants still inhibited c-*fos* promoter activity (about 50%, relative to mock transfectants), but the extent was significantly lower than that of WT

as well as other YF mutants. These results strongly suggest that phosphorylation of Tyr-281 on PTP20 is essential for expression of catalytic activity against not only Tec but also PTP20 itself in transfected COS7 cells as well as in Ramos B cells, although other tyrosine residues, Tyr-303, Tyr-354, and Tyr-381, are also phosphorylated by Tec.

DISCUSSION

Many signaling pathways triggered by PTKs can be potentially modulated by PTPs in a negative or positive manner under cellular context. In some cases phosphorylation on the tyrosine residues of PTPs themselves can modulate their catalytic activities. For example, SH2 domain-containing PTP SHP-2 is tyrosine-phosphorylated upon stimulation by a variety of growth factors (27–29) and cytokines (30–35). Once SHP-2 becomes tyrosine-phosphorylated, their catalytic activity might be increased and modulated its own tyrosine phosphorylation level by autodephosphorylation activity (36, 37). It also has been reported that tyrosine phosphorylation of PTP1B upon insulin and epidermal growth factor treatment causes reduction in its catalytic activity, thereby enhancing apparent insulin receptor- and epidermal growth factor receptor-mediated signaling pathways (38, 39). Thus, tyrosine phosphorylation of PTPs appeared to be critical for the regulation of their biological functions.

Among the PEST family PTPs, PTP20 is an only member that gets phosphorylated on tyrosine residues, whereas no tyrosine phosphorylation of other members, PTP-PEST and PTP-
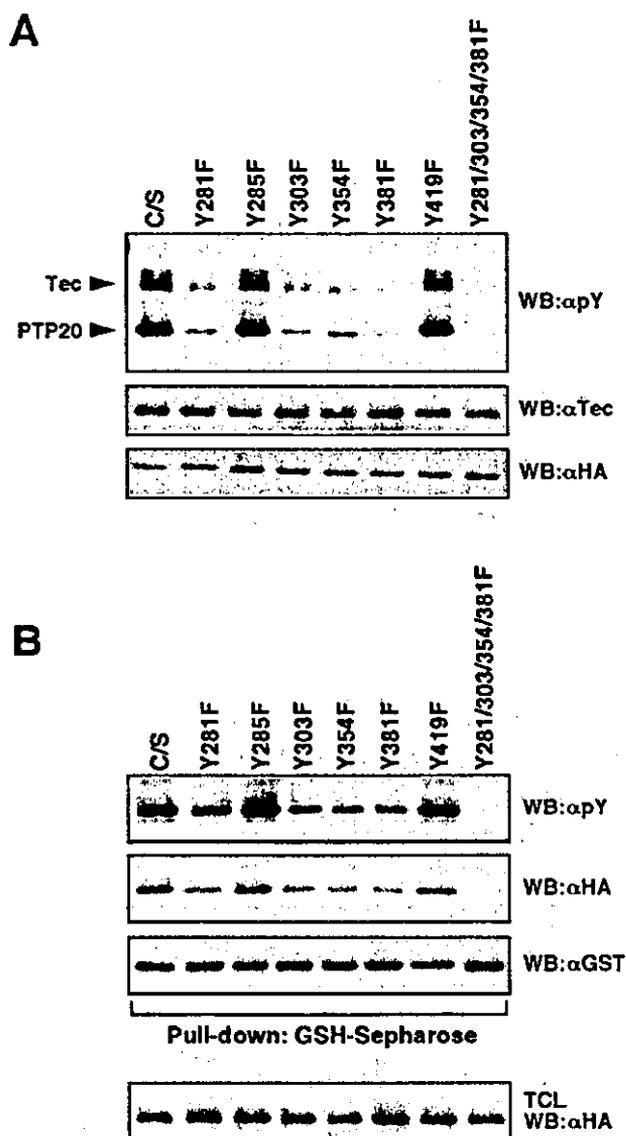
A

B

Pull-down: GSH-Sepharose

FIG. 5. **Specific tyrosine residues of PTP20 are necessary for tyrosine phosphorylation of Tec and association with Tec SH2 domain.** *A*, HA-PTP20 C/S or its YF (tyrosine to phenylalanine substitution) mutants as indicated were co-transfected into COS7 cells with Tec. Aliquots of total cell lysates (*TCL*) were immunoblotted (*WB*) with anti-phosphotyrosine (*apY*) antibody. The same membrane was sequentially reprobed with anti-Tec and -HA antibodies. *B*, COS7 cells were co-transfected with expression plasmids for HA-PTP20 C/S or its YF mutants, Tec, and GST-Tec-SH2 domain. Cells were lysed, and GST-Tec-SH2 domain was precipitated with GSH-Sepharose beads followed by immunoblot analysis by sequential probing with anti-phosphotyrosine, anti-HA, and anti-GST antibodies. Expression of nearly the same amounts of PTP20 was confirmed by immunoblotting of aliquots of total cell lysates with anti-HA antibody.

PEP, has been reported. In the present study, we clearly demonstrated that PTP20 was tyrosine-phosphorylated by a cytosolic Tec kinase. As previously reported for phosphorylation of PTP20 by constitutively active Src family kinases (8, 11), the catalytically inactive form of PTP20 was found to be tyrosine-phosphorylated to a greater extent by Tec, whereas apparently no phosphorylation on PTP20 WT was obvious, possibly due to its autodephosphorylation activity. Src and Lck indeed tyrosine-phosphorylated PTP20, but the extent of tyrosine phosphorylation of PTP20 by Tec was shown to be the greatest (Fig. 1). Moreover, related Itk did tyrosine-phospho-

rylate PTP20 to a lesser extent, but Btk and Bmx did not (Fig. 1). These results suggest that Tec kinase tyrosine phosphorylates PTP20 more specifically and preferentially than Src family kinases and its related kinases do.

Without ectopic PTP20 expression, tyrosine phosphorylation of Tec kinase was not detected in transfected COS7 cells (Fig. 2). Although co-expression of PTP20 WT did not induce tyrosine phosphorylation of Tec, the catalytically inactive C/S variant of PTP20 caused tyrosine phosphorylation of Tec and co-immunoprecipitated with Tec. These results strongly suggest that a dominant-negative effect of PTP20 C/S expression on Tec tyrosine phosphorylation seems to be unlikely and, rather, that Tec was possibly autophosphorylated and further activated by interacting with PTP20 and then was immediately dephosphorylated and deactivated by PTP20, which might also be activated through interaction with Tec in a tyrosine phosphorylation-dependent manner. A deletion of the Tec SH2 domain abrogated tyrosine phosphorylation of Tec as well as PTP20 and association between Tec and PTP20 (Fig. 3). Likewise, substitution of individual tyrosine residues Tyr-281, Tyr-303, Tyr-354, and Tyr-381 with phenylalanines of PTP20 reduced not only tyrosine phosphorylation of Tec and PTP20 itself but also association of PTP20 with the Tec SH2 domain (Fig. 5). Substitution of all the four tyrosine residues (Fig. 5) as well as a deletion of the C-terminal non-catalytic segment (Fig. 6) completely abolished those events, and the C-terminal segment alone partially induced Tec tyrosine phosphorylation (Fig. 6), supporting the idea that phosphotyrosine-dependent interaction between PTP20 and Tec is essential for determining a mutual state of phosphorylation and activation. Taken together, we propose a working hypothesis of tyrosine phosphorylation-dependent interaction between PTP20 and Tec kinase (Fig. 10).

PTPs exhibit elaborate substrate specificity *in vivo*. This specificity can be achieved at two levels. First, the phosphatase catalytic domain itself displays an intrinsic specificity for its substrate. However, the affinity between the catalytic domain and its substrate is often low. Actually, the PTP domain of the catalytically inactive PTP20 alone could not capture a potential substrate Tec kinase (Fig. 6). A further enhancement of the specificity is achieved by protein-protein targeting; the Tec SH2 domain and phosphorylated tyrosine residues on PTP20 could enhance the interaction between the two molecules. In Ramos B cells, we could detect tyrosine phosphorylation-dependent interaction between PTP20 and Tec only when cells were treated with pervanadate (Fig. 7). In this case, however, apparent binding might have resulted from a sole interaction of phosphorylated tyrosines of PTP20 C-terminal with the Tec SH2 domain and, therefore, underestimated because vanadate can get into the catalytic pocket of PTP20 reversibly and inhibit interaction between the PTP domain segment of PTP20 and tyrosine-phosphorylated Tec kinase. Upon physiological stimulation both PTP20 catalytic domain-Tec phosphotyrosine(s) and PTP20 phosphotyrosine-Tec SH2 domain bindings could play an essential role.

Most interestingly, tyrosine phosphorylation of PTP20 appears to regulate its catalytic activity against Tec and PTP20 itself. Among the tyrosine residues phosphorylated by Tec kinase, tyrosine 281 might be critical for dephosphorylation activity of PTP20 in transfected COS7 cells as well as in Ramos B cells (Fig. 9). In the case of ectopic expression in COS7 cells, substitution of the Tyr-281 nearly abolished dephosphorylation activity against both PTP20 and Tec (Fig. 9, *A* and *B*). On the other hand Y281F as well as Y281F/Y303F/Y354/F381F mutants exhibited reduced, but still ~50% dephosphorylation activity as compared with mock transfectants when expressed in
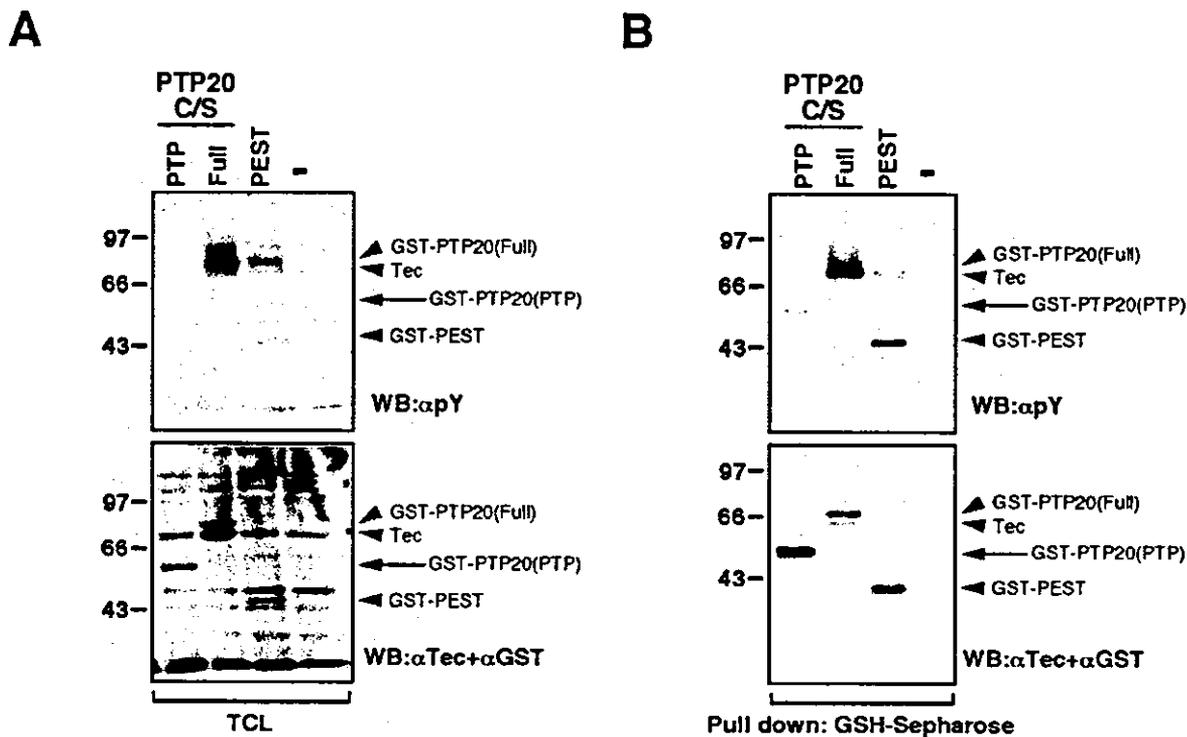
A

B

FIG. 6. **Both PTP catalytic and PEST domains of PTP20 are involved in maximal phosphorylation of Tec and association with Tec.** Tec was co-transfected with either empty pEBG vector (−) or that bearing the PTP20 catalytic domain (*PTP*), full-length PTP20 (*Full*), or the non-catalytic PEST domain of PTP20 (*PEST*). A, aliquots of total cell lysates (*TCL*) were subjected to immunoblotting with anti-phosphotyrosine antibody (*αpY*, *upper panel*). The same membrane was reprobed with a mixture of anti-Tec and anti-GST antibodies. B, remaining cell lysates were precipitated with GSH-Sepharose beads and processed as mentioned above. The bands corresponding to individual products are indicated by *arrows*.
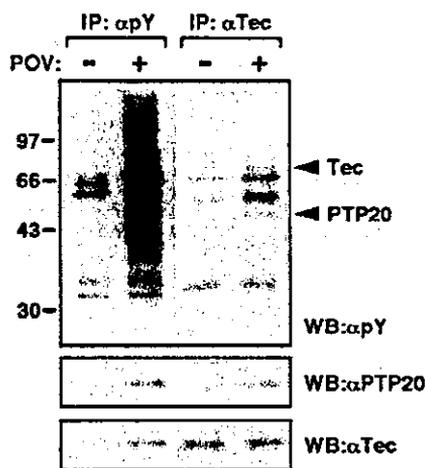
FIG. 7. **Tyrosine phosphorylation-dependent interaction of endogenous PTP20 with endogenous Tec in Ramos B cells.** Ramos cells were treated with 0.1 mM POV for 15 min at 37 °C, lysed, and subjected to immunoprecipitation with either anti-phosphotyrosine (*αpY*) or anti-Tec antibody. The immunoprecipitates (*IP*) were immunoblotted (*WB*) by anti-phosphotyrosine antibody. The same membranes were sequentially reprobed with anti-PTP20 and -Tec antibodies. The bands corresponding to Tec and PTP20 are indicated by *arrowheads*.

FIG. 8. **Negative role of PTP20 in BCR signaling.** Ramos cells (1 × 10⁷) were subjected to electroporation with 2 μg of the pfos/luc reporter plasmid together with 10 μg of pcDNA3 vector (mock) or bearing PTP20 WT, C/S, or D/A mutant. Five hours after transfection cells were incubated for an additional 5 h in the absence (*open bars*) or presence (*closed bars*) of anti-IgM (ab′) (10 μg/ml). Cells lysates were then assayed for luciferase activity. Data are expressed as mean ± S.D. of triplicate determinations.

Ramos B cells (Fig. 9C), suggesting that other direct or indirect mechanisms to regulate PTP20 activity are involved in dephosphorylation and deactivation of Tec in the cells. However, we cannot exclude the possibility that phosphorylation on serine and threonine residues rich in the C-terminal region of PTP20 might affect catalytic activity of PTP20, as PTP20 can be reg-
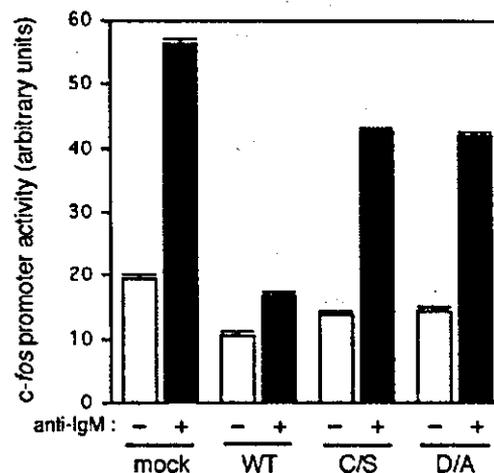
ulated under the control of follicle-stimulating hormone in rat ovarian granulosa cells, where no tyrosine phosphorylation on PTP20 was observed (14).

It has been reported that constitutively active Lck phosphorylates tyrosine residues 354 and 381 on PTP20, which are in turn recognized by the Csk SH2 domain (11). In that report it was also documented that mutation of both the tyrosine resi-
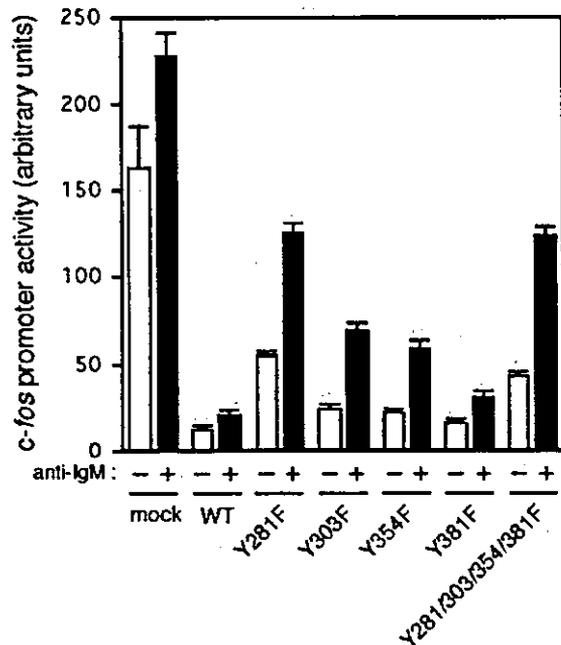
A
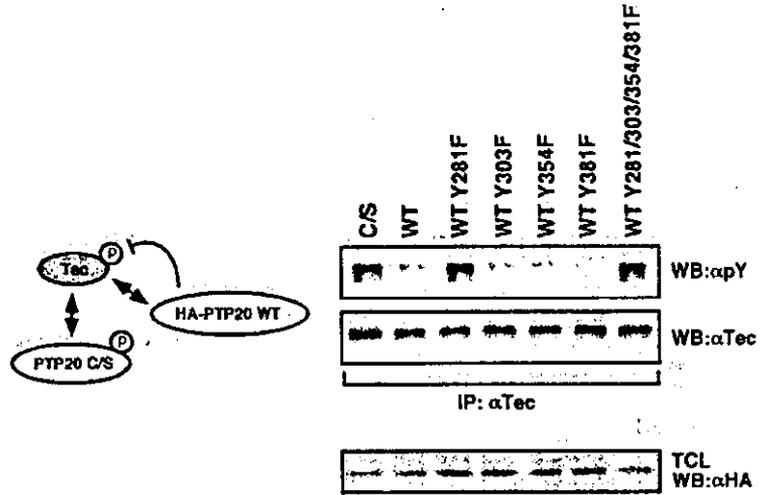
B
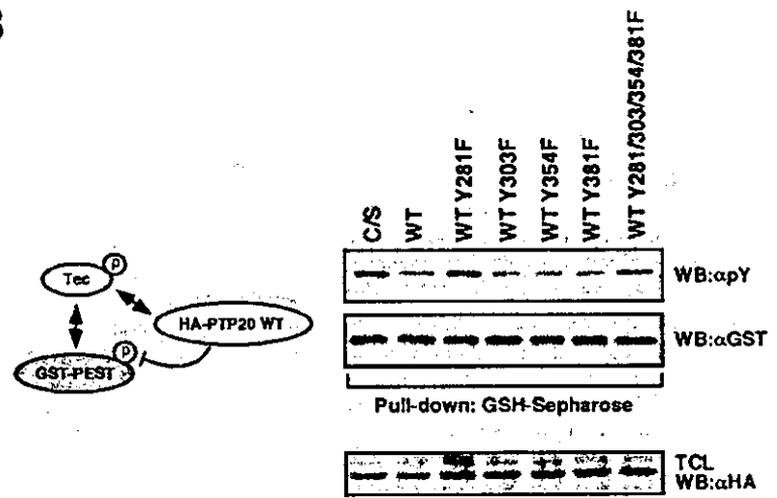
C

FIG. 9. **Tyrosine 281 is critical for** *in vivo* **phosphatase activity of PTP20.** *A*, COS7 cells were co-transfected with Tec, PTP20 C/S, and HA-PTP20 WT or its YF mutants. HA-PTP20 C/S was also included as a negative control. Cells were lysed, and Tec was immunoprecipitated with anti-Tec antibody. The immunoprecipitates (*IP*) were separated by SDS-PAGE followed by immunoblotting (*WB*) with indicated antibodies. Expression of HA-PTP20 was confirmed using aliquots of total cell lysates (*TCL*) with anti-HA antibody. *apY*, anti-phosphotyrosine antibody. *B*, COS7 cells were transfected as above, but PEST-encoding GST-PTP20 PEST domain (GST-PEST) in place of PTP20 C/S was included. Cell lysates were subjected to precipitation with GSH-Sepharose beads and immunoblotted with the indicated antibodies. Expression of HA-PTP20 was confirmed using aliquots of total cell lysates (*TCL*) with anti-HA antibody. *C*, Ramos cells were transfected by electroporation with 2 μg of the pfos/luc reporter plasmid together with 10 μg of pcDNA3 vector (*mock*) or bearing PTP20 WT or its YF mutant and processed as described in legend to Fig. 8.